The infection cushion of Botrytis cinerea : a fungal 'weapon' of plant-biomass destruction

Mathias M. Choquer, Christine Rascle, Isabelle R. Gonçalves, Amélie de Vallée, Cécile Ribot, Elise Loisel, Pavlé Smilevski, Jordan Ferria, Mahamadi Savadogo, Eytham Souibgui, et al.

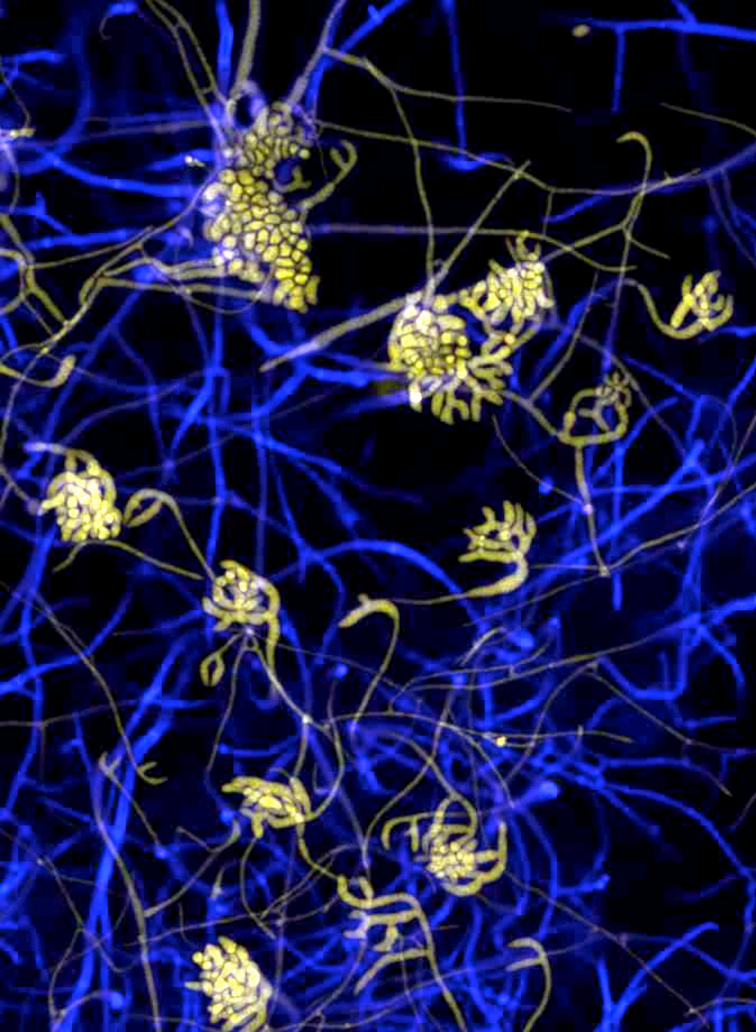

Title: The infection cushion of *Botrytis cinerea*: a fungal "weapon" of plant-biomass destruction

Running title: The infection cushion of *Botrytis cinerea*

Mathias Choquer[1,2*], Christine Rascle[1,2], Isabelle R Gonçalves[1,2], Amélie de Vallée[1,2], Cécile Ribot[1], Elise Loisel[1,2], Pavlé Smilevski[1,2], Jordan Ferria[1,2], Mahamadi Savadogo[1,2], Eytham Souibgui[1,2], Marie-Josèphe Gagey[1,2], Jean-William Dupuy[3], Jeffrey A Rollins[4], Riccardo Marcato[2,5], Camille Noûs[1], Christophe Bruel[1,2*] and Nathalie Poussereau[1,2*]

[1]Univ Lyon, Université Lyon 1, CNRS, INSA-Lyon, Microbiologie, Adaptation et Pathogénie, UMR 5240 MAP, 10 rue Raphaël Dubois, F-69622 Villeurbanne, France ; [2]Bayer SAS, Crop Science Division, Laboratoire Mixte, 14 impasse Pierre Baizet, F-69263 Lyon, France ; [3]Plateforme Protéome, Centre de Génomique Fonctionnelle, Université de Bordeaux, Bordeaux, France ; [4]Department of Plant Pathology, University of Florida, Gainesville, USA ; [5]Department of Land, Environment, Agriculture and Forestry (TESAF), Research Group in Plant Pathology, Università degli Studi di Padova, Legnaro, Italy.

Author for correspondence:

Mathias Choquer

Tel: +33 472852282

Email: mathias.choquer@univ-lyon1.fr

*These authors contributed equally to this work.

Originality-Significance statement

Fungi are the most devastating plant pathogens and the fight against them requires an understanding of their infectious process, and notably the first stages of their infection cycle. Invasion of plants by fungi often involves differentiation of fungal structures called appressoria. Among them, Infection Cushions (IC) are produced by major necrotrophic fungi, such as *Botrytis*, *Sclerotinia*, *Rhizoctonia* and *Fusarium* species. Whether plant penetration would be their only biological role is questionable. Besides, their function at the molecular level is poorly understood. Our paper brings new data about IC of the gray mold causing agent *Botrytis cinerea*, a major worldwide plant pathogen for which identification of new virulence factors and/or new anti-fungal putative targets is of current significance. Based on a transcriptomic study, our work provides molecular information that highlights biological processes specifically at work in mature IC of *B. cinerea*. The gene expression data are supported by a proteomic analysis of the IC secretome, biochemical assays, microscopic observations and mutagenesis of two candidate genes. Firstly, this paper supports the hypothesis that IC are structures dedicated to the massive secretion of effectors important for plant penetration and early necrotrophic invasion, such as phytotoxins, ROS, hydrolytic enzymes and plant cell death-inducing proteins. Secondly, this paper suggests for the first time a role of IC in fungal nutrition. Thirdly, this paper reveals a substantial remodeling of the fungal cell wall in the IC (melanin deposition and chitosan formation) that suggests dynamic modifications at the fungal-host interface likely important for infection. At last, this paper introduces fasciclin-like proteins as new players in *B. cinerea* pathogenesis. In conclusion, our work brings new information about the biology and virulence of this fungus. It could also be of interest to the community working on plant-pathogen interactions.

Summary

The necrotrophic plant-pathogen fungus *Botrytis cinerea* produces multicellular appressoria dedicated to plant penetration, named infection cushions (IC). A microarray analysis was performed to identify genes up-regulated in mature IC. The expression data were validated by RT-qPCR analysis performed *in vitro* and *in planta*, proteomic analysis of the IC secretome and biochemical assays. 1,231 up-regulated genes and 79 up-accumulated proteins were identified. The data support the secretion of effectors by IC: phytotoxins, ROS, proteases, cutinases, plant cell wall degrading enzymes and plant cell death-inducing proteins. Parallel up-regulation of sugar transport and sugar catabolism-encoding genes would indicate a role of IC in nutrition. The data also reveal a substantial remodeling of the IC cell wall and suggest a role for melanin and chitosan in IC function. Lastly, mutagenesis of two up-regulated genes in IC identified secreted fasciclin-like proteins as actors in the pathogenesis of *B. cinerea*. These results support the role of IC in plant penetration but also introduce other unexpected functions for this fungal organ, in colonization, necrotrophy and nutrition of the pathogen.

Introduction

Many phytopathogenic fungi differentiate specific structures named appressoria that are dedicated to the penetration of the host tissues (Emmet and Parbery, 1975; Deising *et al*, 2000). Appressoria facilitate the breaching of plant cuticles and cell walls through a mechanical and/or chemical action. Early microscopy studies provided clear observations of these structures in different fungal species and distinguished unicellular appressoria (UA) from multicellular appressoria, referred to as infection cushions (IC) (Emmet and Parbery, 1975). Later, UA have attracted much attention and molecular understanding of their development and function has tremendously increased (Ryder and Talbot, 2015). In contrast, IC remain far less understood at the molecular level, even if a first transcriptomic study of IC in *Fusarium graminearum* has recently been published (Mentges *et al.*, 2020).

Botrytis cinerea is an ascomycetous fungus that causes grey mould disease on more than 1000 plant species (Elad *et al*., 2016). This disease affects fruits, vegetables and ornamental plants around the world, causing considerable losses every year. It has been ranked among the ten most severe fungal plant pathogens due to its negative impact on agronomically important crops and on plant products in post-harvest storage. *B. cinerea* is considered a typical necrotrophic fungus and has become a model to study plant infection (Dean *et al.*, 2012). It is characterized by its ability to produce either UA or IC *in vitro* or *in planta* (Choquer *et al.*, 2007).

The *B. cinerea* IC are multicellular appressoria that develop *in planta* between 24 h to 48 h after spore germination. Histological studies have revealed IC from *B. cinerea* on a wide variety of infected plant hosts and organs: carrot roots (Sharman & Heale, 1977); bean or mung bean hypocotyls (Garcia-Arenal & Sagasta, 1980; Backhouse & Willets, 1987), bean, cucumber or oilseed rape leaves (Akutsu *et al.*, 1981; Van den Heuvel & Waterreus, 1983; Zhang *et al*., 2010), stone fruit or waxflower flowers (Fourie & Holtz, 1994; Dinh *et al*., 2011), lemon or persimmon fruits (Fullerton *et al*., 1999; Rheinländer *et al*., 2013) and onion epidermis

(Choquer *et al.*, 2007). Lastly, *B. cinerea* IC also develop *in vitro*, in culture over hard surfaces (Backhouse and Willetts, 1987).

IC have been described in several other Leotiomycetes fungi: *Sclerotinia sclerotiorum* (Tariq & Jeffries, 1984), *Sclerotinia minor* (Lumsden & Wergin, 1980), *Sclerotinia trifoliorum* (Prior & Owen, 1964), *Dumontinia tuberosa* (Pepin R, 1980), *Stromatinia cepivora* (Stewart *et al*., 1989) and *Tapesia yallundae* (Daniels *et al*., 1991). In parallel, IC have been described in the Sordariomycetes *Fusarium graminearum* (Boenisch & Schäfer, 2011), and in the Basidiomycota *Athelia rolfsii* (Smith *et al*., 1986), *Rhizoctonia solani* (Demirci & Döken, 1998) and *Rhizoctonia tuliparum* (Gladders & Coley-Smith, 1977).

The recent characterization of several avirulent mutants of *B. cinerea* revealed the importance of IC in the infectious process of this necrotrophic fungus (De Vallée *et al*., 2019) and hypovirulent strains of *B. cinerea* infected by mycoviruses are also deficient in IC formation (Zhang *et al*., 2010; Hao *et al*., 2018). Although it has long been accepted that IC mediate penetration, their differentiation as well as their functions are still poorly understood. By using a transcriptomic approach, the aim of this study was to provide new molecular information that highlights biological processes specifically at work in mature IC of *B. cinerea*.

The transcriptomic results, supported by a secretome analysis, are consistent with IC being structures dedicated to the secretion of fungal effectors important for plant penetration and colonization: phytotoxins, ROS, hydrolytic enzymes and plant cell death-inducing proteins. Moreover, the data reveal a deep remodeling of the IC cell wall composition suggesting the importance of melanin and chitosan in the function of IC. The hypothesis of a role for IC in the nutrition of the parasite is also proposed.

Results

Microarray study of IC

To gain information on the role of IC in the biology of *B. cinerea*, we identified genes expressed in these structures. As IC develop onto solid surfaces, potato dextrose agar plates were used for their production while potato dextrose broth was used to produce the control vegetative mycelium. Conidia were used as inoculum, and cellophane sheets were overlaid onto the plates to increase the production of IC and to facilitate their harvest. To obtain as much mature IC as possible, the samples were collected at 44 hpi. At that time, IC were fully differentiated and hyperbranched (Fig. 1), and they covered about 40% of the plates surface (Fig. S1a) while the liquid cultures produced only mycelium (Fig. S1b). Both biological materials were used to extract total RNA and to prepare cDNAs that were hybridized to microarrays carrying probes of 11,134 *B. cinerea* genes (Table S1).

Data processing, quality controls and differential expression analysis of the microarrays data led to the listing of 1,231 up-regulated genes and 1,422 down-regulated Bcin genes (fold change ≤ -2 or ≥ 2; FDR < 0.05; Table S1) in the IC-enriched sample (hereafter referred to as IC) when compared to the control vegetative mycelium (13% and 15% of the 9,410 expressed genes, respectively). The reliability of this result was tested by RT-qPCR analysis. For this, new IC and new control mycelium were produced in order to extract new RNAs. The RT-qPCR reactions were run on 39 genes selected among the up-, down- and non-regulated genes identified by the microarray study (the selection covered genes with different fold-changes). The results confirmed the microarrays data in 85% of the cases (33 genes) and showed no contradiction with the transcriptomic data in the remaining 15% of the cases (Table S2). Altogether, this granted the microarray data a good level of confidence.

Functional enrichment analysis of differentially expressed genes in IC

Enrichment analyses was performed on the up- and down-regulated genes in IC. By using the GO biological process classification (Gene Ontology; Fig. S2), a significant enrichment was revealed for carbohydrate metabolic process (58 genes), oxidation-reduction process (136 genes), metabolism process (70 genes), transmembrane transport (76 genes) and proteolysis (24 genes). For down-regulated genes, rRNA processing (15 genes), ribosome biogenesis (9 genes) and tRNA splicing (5 genes) showed enrichment. In order to extract biological meaning from the GO analysis, we used existing databases and published data to manually sort the transcriptional data into 22 functional subcategories (Table S1). Fisher's exact tests confirmed the enrichment of 18 subcategories relating to virulence: plant degradation, production of phytotoxins (and other secondary metabolites) and ROS, plant cell death induction, and fungal cell wall remodeling, nutrition and secretion (Table 1).

Fungal protein effectors: enzymes degrading the plant tissues and plant cell death-inducing proteins

The carbohydrate-active enzymes database (CAZy, Lombard *et al.*, 2014) and the classifications of Plant Cell Wall Degrading Enzymes (PCWDE; Van den Brink & de Vries, 2011; Glass *et al.*, 2013) were used to subclassify 126 predicted PCWDE-encoding genes in *B. cinerea* according to their putative specificity for cellulose (C), hemicellulose (H), pectin (P) or overlapping specificity (H, P or C) (Table S1). As shown in Table 1, genes coding for hemicellulases, pectinases, and PCWDE of overlapping specificity were significantly enriched among the up-regulated genes in IC, while the genes coding for cellulases were not. Genes coding for cutinases and proteases were also found significantly enriched among the up-regulated genes in IC (Table 1). In particular, the aspartyl proteases (Ten Have *et al*., 2010), sedolisins and metallopeptidases subcategories were enriched. Altogether, these results suggest a role for IC in the

157 degradation of the plant barriers and tissues through the production and secretion of hydrolytic
158 enzymes.
159 In addition, 6 genes encoding plant cell death-inducing proteins (CDIP; Li *et al.*, 2020) were
160 up-regulated in IC: *BcPg2* and *BcPg3* (Kars *et al.*, 2005), *BcXyn11A* (Brito *et al.*, 2006),
161 *BcNep2* (Schouten *et al.*, 2008), *BcXyg1* (Zhu *et al.*, 2017) and the homolog of VmE02 (Nie *et*
162 *al.*, 2019). The subcategory of CDIP is significantly enriched among the up-regulated genes in
163 IC (Table 1) and this would suggest that IC actively participate in the triggering of plant cell
164 death.
165
166 **Fungal small molecule effectors: phytotoxins and reactive oxygen species (ROS).**
167 Detailed examination of the predicted 42 genes that code for Secondary Metabolism (SM) key
168 enzymes in *B. cinerea* B05.10 strain (Table S1; Collado & Viaud, 2016) showed that 11 were
169 up-regulated in IC (Table 1; Fig. S3). Noticeably, two SM gene clusters, responsible for the
170 production of botcinic acid and botrydial phytotoxins (Dalmais *et al.*, 2011; Porquier *et al.*,
171 2019), were both significantly enriched among the up-regulated genes in IC (subcategories "10"
172 and "11" in Table S1; Table 1; Fig. 2a). In addition, the *Bcreg1* gene (Bcin03g07420) encoding
173 the transcriptional regulator required for the synthesis of these toxins (Michielse *et al.*, 2011)
174 was also up-regulated (Table S1). At last, we observed that five remaining up-regulated SM
175 key enzyme-encoding genes are neighbored by genes whose expression was also up-regulated
176 in IC, and whose description is compatible with SM typical genes (Fig. S4). This suggests the
177 existence of four additional putative SM clusters transcriptionally induced in *B. cinerea* IC.
178 These gene clusters include the *Bcdtc3*, *Bcpks7*, *Bcpks8* or *Bcpks4*/*Bcnrps8* genes.
179 Detailed examination of the predicted 54 genes that code for ROS producing systems in *B. ci-*
180 *nerea* (Siegmund & Viefhues, 2016) showed that 14 were up-regulated in IC, making this gene
181 family an enriched subcategory (Table 1; Table S1). These genes encode the catalytic subunit

BcNoxB of the NADPH oxidase and its regulator BcNoxR (Segmüller *et al.*, 2008), the glucose oxidase BcGod1 (Rolke *et al.*, 2004), the galactose oxidase BcGox1, the quinone oxidoreductase BcNqo1 (An *et al.*, 2016), as well as 3 laccases (BcLcc6, 8, 13) and 6 glucose-methanol-choline (GMC) oxidoreductases. As ROS play a role in the early phases of plant infection by *B. cinerea* (Govrin and Levine, 2000), up-regulation of these genes suggested that IC could secrete more ROS than vegetative mycelium. To test this hypothesis, *B. cinerea* was cultured for 48 h on liquid PDB medium overlaid with cellophane sheets and the collected culture medium was exposed to 3,3' diaminobenzidine (DAB) as previously described (Viefhues *et al.*, 2014). In comparison with the vegetative mycelium, a stronger oxidation of DAB was observed with the IC-culture medium (Fig. 2b), indicating the presence of likely higher H_2O_2 concentration and secretion of peroxidase activity.

Melanization and chitin deacetylation remodel the fungus IC cell wall

In *B. cinerea*, dihydroxynaphthalene-(DHN)-melanins are produced and their biosynthesis relies on a bipartite pathway operating in conidia or in sclerotia (Schumacher, 2016). In conidia, the genes coding for the polyketide synthase BcPks13 and for the hydrolase BcYgh1 are induced by the light transcription factor BcLft2. In sclerotia, the polyketide synthase BcPks12 encoding gene is induced by the transcription factor SMR1 and repressed by BcLtf2 (Cohrs *et al.*, 2016). In IC, *Bcpks13*, *Bcygh1*, *Bcltf2* and the other downstream genes of the pathway were up-regulated while *Bcpks12* and *Bcsmr1* were down-regulated (Fig. 3a-c). This would indicate that IC produce DHN-melanins by using the biosynthetic pathway at play in conidia. Schumacher (2016) proposed laccases as potential candidates catalyzing the polymerization of DHN-melanins monomers in *B. cinerea*. As *BcLcc6* and *BcLcc8* laccases genes are up-regulated in IC, they could eventually play this role (Sapmak *et al.*, 2015). In addition, thick dark cell walls were observed in IC (Fig. 3d, top), suggesting that DHN-melanins are deposited at

the contact zones between the hyperbranched IC lobes. In the presence of tricyclazole, an inhibitor of the THN reductases BcBrn1 and BcBrn2 (Fig. 3b), hyperbranched IC lobes were still formed but their dark cell walls were not visible anymore. Orange cell walls were observed instead (Fig. 3d, bottom), likely due to accumulation of T4HN and T3HN and their autooxidation products flaviolin and 2-hydroxyjuglone (Schumacher, 2016). These results confirm the hyper-melanization of IC cell walls and suggest that melanization and hyperbranching are independent processes.

Chitin deacetylases (CDA) are enzymes that produce chitosan from chitin (Fig. 4a). Based on conserved protein motifs identified in CDAs (Liu *et al.*, 2017), the genome of *B. cinerea* putatively encodes five CDA (data not shown). Three of these genes were up-regulated in IC when compared to the control mycelium (Fig. 4b; Table S1) while *in planta* RT-qPCR analysis showed up-regulation of these 5 genes at the early phase of bean leaves infection (Fig. 4c). Whether the up-regulation of CDA genes impacted the IC cell walls was addressed by using confocal microscopy and differential staining of chitin and chitosan. This allowed the specific visualization of chitosan in IC, hooks and their generating hyphae, but not in the vegetative mycelium (Fig. 4d). This result confirms that some chitin is converted into chitosan in the IC cell wall.

Up-regulation of sugar uptake and catabolism in IC

The “Sugar transporters” subcategory was explored by mining the BotPortal database (http://botbioger.versailles.inra.fr/botportal) using the four InterPro domains IPR003663, IPR005829, IPR007271, and IPR004689. This led to the listing of 86 predicted sugar transporters in the genome of *B. cinerea* (Table S1), among which 22 were up-regulated in IC (Table 1). This up-regulation suggests a possible activation of the sugar catabolic pathways and, noticeably, two genes of the glycolysis pathway were up-regulated in IC, coding for the fructose-

bisphosphate aldolase (Bcin07g03760; Table S1) and the glucose-6-phosphate isomerase *Bcpgi* (Bcin15g04970; Table S1). Besides, in the gluconeogenesis pathway, the *BcPck1* gene (Bcin16g00630; Table S1) encoding the phosphoenolpyruvate carboxykinase was also up-regulated in IC. Liu *et al*. (2018) showed that this key gene is crucial for *B. cinerea* virulence and for the formation of IC in the absence of glucose. In addition to the enriched metabolic pathways that relate to the degradation of polysaccharides (pectin, glycans), these results suggest an activated sugar catabolism in IC.

IC secretome analysis validates the transcriptome analysis

Of the 1,231 up-regulated genes in IC, 266 were predicted to code for putative secreted proteins with a N-terminal signal peptide (Table 1 and Table S1) To further investigate this data, the secretomes of IC and control mycelium were compared. *B. cinerea* was grown on cellophane sheets overlaying potato dextrose broth and the culture media were collected at 24 h (control mycelium) or at 48 h when IC covered ~40% of the cellophane surface. The proteins were extracted and subjected to a comparative and quantitative proteomics analysis. 79 proteins identified in 3 biological replicates with a minimum of 2 unique peptides were listed as up-accumulated (Fold change ≥ 3, FDR < 0.05) in IC (Table 2 and Table S3). Comparison of the proteomics and microarray data (Table S3) showed that 40 of the up-accumulated proteins (51%) are encoded by genes up-regulated in IC. By using the GO biological process classification, we observed that these secreted proteins are essentially involved in carbohydrate and polysaccharide metabolic processes (27 proteins), proteolysis (16 proteins), oxidation-reduction process (12 proteins), and other metabolic process (2 proteins). All these GO categories were found enriched in the analysis of the genes up-regulated in IC (Fig. S2). We then used existing databases and published data to manually sort the proteomics data into functional subcategories. We identified virulence-related subcategories similar to those issued from the transcriptome

analysis: degradation of plant cuticle, plant cell wall and starch, production of ROS, other degrading enzymes (e.g. nucleases, phosphatases and esterases) and plant cell death-inducing proteins. Besides, six CDIP were up-accumulated in the secretome of IC: BcXyn11A (Brito *et al*., 2006), BcNep2 (Schouten *et al.*, 2008), BcSpl1 (Frias *et al*., 2013), BcGs1 (Zhang *et al*., 2015), BcIeb1 (Frias *et al*., 2016) and BcXyg1 (Zhu *et al.*, 2017). Lastly, a new subcategory enriched in the IC secretome could be identified that corresponds to fungal enzymes implicated in the crosslinking of cell wall polysaccharides. This suggests possible modifications of the covalent links between chitin, glucans and proteins of the IC cell wall. Altogether, the proteomics data support the transcriptomic data and strengthen the signatures of cell wall remodeling and secretion of hydrolytic enzymes or effectors.

Relevance of the microarray data to plant infection

Fourteen up-regulated genes in IC whose predicted function relates to pathogenesis were selected for a time course RT-qPCR analysis *in planta* (bean leaves infected with conidia of *B. cinerea*; Fig. 5a and 5b). All the selected genes were expressed *in planta* suggesting that the microarray data are relevant to plant infection. Twelve of the studied genes were up-regulated at days 2, 3 and/or 4 of infection, when IC were visible at the leaf surface. When only hooks could be observed (day 1), most of these genes (11) were not expressed. Furthermore, expression peaked at day 2 for 7 genes, when IC were visible, but plant tissue maceration was not. These results suggest that these genes expressed early in IC could play a role in events triggering plant cell death.

Fasciclin-like genes up-regulated in IC are actors in the virulence of *B. cinerea*.

Fasciclins play a role in the virulence of the rice pathogen *M. oryzae* (Liu *et al.*, 2009) via a possible role in development or in autophagy (Seifert, 2018). In *B. cinerea*, two genes encode

fasciclin-like proteins (*Bcflp1*; Bcin04g05020 and *Bcflp2*; Bcin09g05010) and both these genes were up-regulated in IC. Following confirmation of this differential expression by RT-qPCR *in vitro* and *in planta* (Table S2; Fig. 5), and since BcFlp1 was up-accumulated in the secretome of IC (Table 2 and Table S3), these two genes were selected for mutagenesis. By using a gene replacement strategy, single mutant strains (Δ*Bcflp1* and Δ*Bcflp2*) and the double mutant strain (Δ*Bcflp1::*Δ*Bcflp2*) were constructed. These mutants were genetically purified, and the genotypes were verified by PCR and Southern blotting (Fig. S5). Two independent transformants of each mutant were then characterized. IC formation could be observed in all mutants (data not shown), indicating that the two fasciclin-like proteins are not required for the differentiation of hyphae into IC in *B. cinerea.* By contrast, bean leaves infection assays showed that the mutants were affected in their pathogenesis (Fig. 6a-b). In the Δ*Bcflp1* mutant, the colonisation rate was similar to that of the wild type, but apparition of the symptoms was delayed (estimated at 12h). In the Δ*Bcflp2* and Δ*Bcflp1::*Δ*Bcflp2* mutants, the colonisation rate was reduced and stopped after 4 days. Noticeably, a dark ring was visible at the periphery of the macerated tissues. *In vitro*, neither *Bcflp1* or *Bcflp2* deletion impaired hyphal growth on rich medium (data not shown). On minimal medium, the Δ*Bcflp2* and Δ*Bcflp1::*Δ*Bcflp2* mutants were moderately impaired in hyphal growth, but the Δ*Bcflp1* mutant was not (Fig. 6c). Altogether, the data could indicate that Bcflp1 plays a role during the early stage of the infection process while Bcflp2 could play a role at a later stage. At last, the phenotype of the double mutant indicates a dominant effect of the Δ*Bcflp2* mutation over Δ*Bcflp1*.

Discussion

A role of IC in plant penetration and potentially in nutrition.

In plant pathogenic fungi, IC have been proposed to play an important role in host penetration. In this study, four cutinase-encoding genes and 48 predicted PCWDE-encoding genes were revealed as up-regulated in *B. cinerea* IC. These genes include the endopolygalacturonase *BcPg2* (Bcin14g00610), the endoxylanase *BcXyn11A* (Bcin03g00480), and the endoarabinanase *BcAra1* (Bcin02g07700) required for full virulence of *B. cinerea* (Kars *et al*., 2005; Brito *et al*., 2006; Nafisi *et al*., 2014). Besides, aspartyl proteases, sedolisins and metallopeptidases-encoding genes were also significantly up-regulated. A proteomic analysis of IC secretome confirmed the up-accumulation of CAZymes and proteases when compared to vegetative mycelium. Altogether these results support a role for IC in host penetration *via* enzymatic degradation of plant cell walls.

Unexpectedly, 25 genes coding for sugar transporters and sugar metabolic enzymes were up-regulated in IC. In connection with the up-regulation of PCWDE-encoding genes, this suggests that IC could play a role in nutrition by importing and catabolizing sugar molecules originating from plant polysaccharides degradation. This would compare to the unicellular appressorium of the rice pathogen *M. oryzae* which, besides plant penetration, would also serve to feed on host plant carbohydrates (Soanes *et al.*, 2012).

A role of IC in establishing necrotrophy ?

Two known SM gene clusters are up-regulated in IC. These clusters are responsible for the production of botcinic acid and botrydial, two phytotoxins playing a role in plant infection by *B. cinerea* (Cutler *et al.*, 1993 & 1996; Deighton *et al.*, 2001; Dalmais *et al.*, 2011; Massaroli *et al*., 2013; Collado & Viaud, 2016). Botrydial sesquiterpene and its derivatives botryanes are proposed as fungal effectors manipulating plant host defenses, promoting cell death and thus

enabling *B. cinerea* to feed on necrotic tissues (Rossi *et al*., 2011). Botcinic acid polyketide and its structurally related botcinins and botrylactones cause plant chlorosis and necrosis (Cutler *et al*., 1993). Double inactivation of these SM clusters led to a defect of pathogenesis and demonstrated the concerted action of the two toxins (Dalmais *et al*., 2011). Interestingly, the co-expression of these clusters in IC supports this concerted action. In addition, four putative SM clusters were also up-regulated in IC. The role these clusters might play in virulence and the putative metabolites produced as a result of their activation await characterization. It is noteworthy that several orphan SM have been reported in *B. cinerea* while their biosynthesis genes remain unknown (Collado and Viaud, 2016). Additionally, it was proposed that secretion of new sesquiterpenoid metabolites, called eremophilenols, could promote and regulate the production of *B. cinerea* IC, perhaps acting as an endogenous signal (Pinedo *et al*., 2016).

During the early phase of plant-fungal interaction, plants produce ROS as part of their defense mechanisms, but ROS are also produced by the pathogen as cell death inducers. In order to produce and to cope with ROS, *B. cinerea* is equipped with multiple oxidoreductases. Chemical compounds or mutations that target some of these enzymes, or their encoding genes, impair virulence (Rolke *et al*., 2004; Segmüller *et al*., 2008; An *et al*., 2016; Siegmund & Viefhues, 2016). The analysis of the up-regulated genes in IC highlighted 136 genes related to the oxidation-reduction process, among which 15 genes coding for putative ROS producing enzymes. In addition, higher levels of H_2O_2 were detected in IC culture media compared to vegetative mycelium control media. This suggests that IC secretes high amounts of ROS and would therefore be consistent with the production of ROS observed in IC during penetration of onion epidermis (Choquer *et al*., 2007; Marschall & Tudzynski, 2016b). Several gene mutations which impair IC formation in *B. cinerea* have been identified in recent years. Interestingly these genes are often associated with oxidoreduction processes and play a role in the development and virulence of *B. cinerea*. These genes encode the regulator of oxidative stress response BcSkn7 (Viefhues

et al., 2015), the scaffold protein BcIqg1 involved in resistance against oxidative stress (Marschall and Tudzynski, 2016a), the aquaporin BcAqp8 involved in ROS production (An *et al*., 2016), the ER protein BcPdi1 involved in redox homeostasis (Marschall and Tudzynski, 2017) and the H3K4 demethylase BcJar1 orchestrating ROS production (Hou *et al*., 2020).

During the early phase of plant infection by *B. cinerea*, cell death inducing proteins (CDIP) (Qutob *et al.*, 2007; Cuesta Arenas *et al.*, 2010) could trigger plant cell death from which the fungus would benefit to achieve full virulence (Govrin and Levine, 2000; Govrin *et al.*, 2006). Up-regulation of CDIP-encoding genes and/or secretion of CDIP have been recorded in *B. cinerea* (Shlezinger *et al.*, 2011; González *et al.*, 2016; Noda *et al*., 2010; Zhu *et al*., 2017). Our study reveals gene up-regulation and/or protein up-accumulation for 9 of the 14 known CDIPs in *B. cinerea*. Altogether, the up-regulation of genes involved in the production of CDIP, phytotoxins and ROS argues for IC playing a role in the establishment of the necrotrophic lifestyle of *B. cinerea*.

In *Colletotrichum* unicellular appressoria, genes encoding effectors and secondary metabolism enzymes are induced before penetration and during biotrophy while genes encoding most hydrolases and transporters are up-regulated later, at the switch to necrotrophy (O'Connell *et al.*, 2012). In comparison, the concomitant expression of all these genes recorded herein could also support a role of *B. cinerea* IC in necrotrophy.

Cell wall remodeling in IC.

In *B. cinerea*, cell walls are darkened by DHN-melanins. These pigments are secondary metabolites produced via a bipartite pathway in *B. cinerea*, so far identified as specific to conidia or sclerotia (Schumacher, 2016). The gene expression data reported in this study indicate that the conidial metabolic pathway is activated in IC, while the sclerotial pathway is not. This result suggested that IC produce melanin, as observed in unicellular melanized appressoria (Soanes,

2012). Microscopic observation of thick dark cell walls in IC that are sensitive to DHN-melanins inhibitors brought experimental support to this. Melanins biosynthesis is dispensable for virulence in *B. cinerea* (Schumacher, 2016) and the reason of their increased production in IC remains to be clarified. It could play a role in the fungus survival during the oxidative burst of host plants (Govrin and Levine, 2000), but it could also play a role in the cross-linking of cell wall components (Franzen *et al.*, 2006), the binding of proteins (Mani *et al.*, 2001) or that of metals (Fogarty and Tobin, 1996).

Three genes coding for chitin deacetylases (CDA) are up-regulated in IC. Moreover, differential staining of chitin and chitosan allowed microscopic observations of chitosan in IC and not in vegetative hyphae. This indicates that some chitin is deacetylated into chitosan in the cell wall of IC. Since CDA can play a role in *Aspergillus fumigatus* polar growth (Xie *et al.*, 2020) or in *Magnaporthe oryzae* appressorium differentiation (Kuroki *et al.*, 2017), the transformation of chitin into chitosan in *B. cinerea* might be involved in the change of hyphal growth that leads to IC formation. Alternatively, the production of chitosan by CDA could play a role in cell wall anchoring of melanins, cell wall integrity, osmotic stability, modulation of extra-cellular polysaccharide production and/or adhesion to surfaces (Baker *et al.*, 2007; Geoghegan and Gurr, 2016; Perez-Dulzaides *et al.*, 2018; Chrissian *et al*., 2020). At last, chitin deacetylation could prevent detection by the host immune system (Cord-Landwehr *et al.*, 2016; Upadhya *et al*., 2018; Lam *et al*., 2019).

Another cell wall-related gene up-regulated in *B. cinerea* IC is *Bcsun1* (Bcin06g06040), a beta-glucosidase-encoding gene that is required for full production of IC and full virulence of *B. cinerea* (Pérez-Hernández *et al*., 2017). This adds to the up-regulation of the DHN melanin-biosynthesis and the CDA genes, and to the up-accumulation of 7 fungal cell wall polysaccharides cross-linking enzymes in the IC secretome. Altogether, this argue for a remodeling of the cell wall in IC.

Evidencing new putative virulence factors from the IC transcriptome.

Based on the up-regulation of their encoding genes in IC, a two-member family of fasciclin-like proteins was selected for functional study. Plant colonisation was respectively delayed and arrested in the *Bcflp1* and *Bcflp2* deletion mutants. This suggests a role for these genes in the infection process of *B. cinerea*, at an early stage for *Bcflp1* and at a later stage for *Bcflp2*. As fasciclins could be involved in autophagy in *M. oryzae* and *Schizosaccharomyces pombe* (Liu *et al*., 2009; Sun *et al*., 2013), one may hypothesize a similar function for BcFlp1 and/or BcFlp2, but this needs to be explored.

In a recent study, we collected transcriptomic and proteomic data from four non-pathogenic mutants of *B. cinerea* that do not produce IC (De Vallée *et al*., 2019). Comparison of these data to those presented here showed that 40 of the first 100 up-regulated genes in IC are down-regulated in all 4 mutants (Fig. S6). In addition, 47% of the proteins up-accumulated in the culture medium of IC are down-accumulated in the secretome of the 4 IC-deficient mutants (Table S3). These genes and proteins represent a list of potential virulence factors/effectors in *Botrytis cinerea.*

Concluding remarks

This *in vitro* study of IC revealed several enriched categories of up-regulated genes (CAZymes, putative effectors, secondary metabolism, ..) that were highlighted in dual-transcriptomes of *B. cinerea* infecting lettuce, tomato, grapevine, cucumber or *Arabidopsis* (Blanco-Ulate *et al*., 2014; Kelloniemi *et al*., 2015; Kong *et al*., 2015; Zhang *et al*., 2019; Zhang *et al.*, 2020). It is therefore relevant to plant infection by *B. cinerea.* Interestingly, the recent transcriptome analyses of *F. graminearum* IC developed *in planta* also showed an enrichment of the same

categories of genes (Mentges *et al.*, 2020), and suggests that IC might share conserved virulence functions in different plant pathogenic fungi.

Experimental Procedures

Fungal strains and growth conditions

Botrytis cinerea B05.10 conidia were collected in PDB medium (Difco) diluted ¼ (PDB¼), after ten days of culture on malt sporulation medium, at 21°C under near-UV light. All subsequent cultures were done in the dark at 21°C. For infection cushions formation, 2.10^5 conidia were spread onto cellophane sheets overlaying PDB¼ medium supplemented with agar (25 $g.l^{-1}$), and the plates were incubated for 44 h. For the control sample, 2.10^5 conidia were inoculated in 50 ml PDB¼ medium and the 250 ml-flasks were agitated (110 rpm) for 44 h. The flasks were previously siliconized with Sigmacote (Sigma) to prevent mycelium adhesion and IC formation on the glassware. For radial growth measurements, wild-type and mutant strains were grown on minimal medium ($NaNO_3$ 2 $g.l^{-1}$, Glucose 20 $g.l^{-1}$, KH_2PO_4 0.2 $g.l^{-1}$, $MgSO_4$, $7H_2O$ 0.1 $g.l^{-1}$, KCl 0.1 $g.l^{-1}$, $FeSO_4$, $7H_2O$ 4 $mg.l^{-1}$). For secretome analysis, 2.10^5 conidia were spread onto cellophane membrane overlaying solid PDB¼. After 6 h incubation (21°C), membranes were transferred on 2 ml liquid PDB¼ for 24h (Control mycelium condition) or 48 h (IC condition) at 21°C. Liquid medium was then collected for proteomic analysis. For micrsocopy, 10^4 conidia or single mycelial plug served to inoculate PDB¼ medium in 6-wells microplates (). The plates were incubated 44h at 21°C in the dark.

Microarray expression analysis

To study the transcriptome of *B. cinerea*, NimbleGen 4-plex arrays containing 4 x 72,000 arrays per slide were used (Roche, Mannheim, Germany). Construction of this chip was initially based on combining two previous genome annotations (Amselem *et al*., 2011), the one of the T4 strain by URGI (BofuT4 gene references; www.urgi.versailles.inra.fr) and the one of the B05.10 strain by the Broad Institute (BC1G gene references; www.broadinstitute.org). Thus, 62,478 60-mer oligonucleotides were designed as specific probes covering 20,885 predicted gene

models and non-mapping Expressed Sequence Tags (EST) (3 oligonucleotides per gene or EST) and 9,559 random probes were designed as negative controls.

The structural annotation used for this study was published by van Kan *et al.* (2017), displaying 11,710 predicted genes, associated to 13,749 predicted proteins, unlike the two previous annotations showing more than 16,000 predicted genes (BofuT4 and BC1G). This annotation is considered better on the basis of RNA-seq data and is available at EnsemblFungi under the reference *Botrytis cinerea* B05.10 (ASM83294v1; Bcin gene references; http://fungi.ensembl.org/Botrytis_cinerea/). 11,710 Bcin genes are predicted but not all of them were analyzed by the *B. cinerea* NimbleGen 4-plex arrays. In order to associate each BofuT4 and BC1G gene from the chip to only one Bcin gene and reciprocally, we used the correspondence established in the *B. cinerea* Portal (Simon & Viaud, 2018; http://botbioger.versailles.inra.fr/botportal/). In a hundred of cases, BofuT4/BC1G genes showing correspondence with multiple Bcin genes were checked by gene synteny. After this manual curation, we identified 11,630 BofuT4/ BC1G genes out of 15,750 showing correspondence with only one Bcin gene. When a Bcin gene showed correspondence with multiple BofuT4/ BC1G genes, we selected the BofuT4 or BC1G gene giving the highest normalized intensities. After these two manual curations, we found that 11,134 Bcin genes were analyzed by the chip which represent 95% of the published Bcin genes (11,710; Table S1). The EST and the small coding sequences (< 100 amino acids) lacking EST support were excluded from our analysis.

Total RNA was extracted from 4 mg of ground lyophilized material using the RNeasy Midi kit (Qiagen). A DNase treatment (Ambion) was performed to remove traces of genomic DNA. RNA profiles were assessed using the Bioanalyzer RNA 6000 Nano kit (Agilent). Ten micrograms of total RNA were converted into cDNA using the SuperScript II cDNA Conversion Kit (Invitrogen). Double stranded cDNAs were then labelled with Cy3-nonamers using NimbleGen One-Color DNA Labeling Kit before hybridization on the NimbleGen 4-plex

arrays. Microarrays were then scanned with an Agilent scanner at 532 nm (Cy3 absorption peak) optimized for Nimblegen 4-plex arrays. All steps were performed following the procedures established by NimbleGen. The entire microarray data set described in this article is available at the Gene Expression Omnibus (GEO) database under accession number GSE141822.

Data processing, quality controls, differential expression analysis and clustering were performed using ANAIS methods (Simon and Biot, 2010). Hybridization signals of all probes, comprising three and four independent replicates for mycelium condition and infection cushion condition, respectively, were subjected to RMA-background correction, quantile normalization, and gene summarization. Thresholds of gene expression were determined by referring the hybridization signals to those of 9,559 random probes, calculated for each array using the R software (R Core Team, 2019). Genes were considered expressed when their normalized intensity was higher than the 99th percentile of random probes hybridization signals in at least one biological replicate. These genes were kept for differential expression analysis. Differentially expressed genes, between the infection cushion condition and the mycelium condition, were identified using a one-way ANOVA test. To deal with multiple testings, the ANOVA p-values were submitted to a False Discovery Rate correction (FDR). Transcripts with a corrected p-value <0.05 and for which a fold change ≤ -2 or ≥ 2 was observed between the two conditions were considered to display significant differential expression. Clusters analyses of gene normalized intensities were performed to highlight differentially expressed genes.

Enrichment analysis and genes categorization

Further analyses were performed to highlight biological processes potentially enriched in the selected lists of up-regulated or down-regulated Bcin genes in infection cushion. Enrichment in Gene Ontology (GO) Biological Process (BP) terms was assessed on the *Botrytis cinerea* B05.10 (ASM83294v1) species using the Fungifun website (Priebe *et al.*, 2015; https://elbe.hki-jena.de/fungifun/). The background dataset of genes used as reference was the

11134 Bcin genes which were associated to the chip (Table S1). Presence of a putative signal peptide was predicted using the SignalP 5.0 Server (Almagro Armenteros *et al.*, 2019). The CAZy database (www.cazy.org) was used for the manual curation of plant cell wall degrading enzymes and the alpha-1,2-mannosidases. The InterPro database (www.ebi.ac.uk/interpro/; Mitchell *et al.*, 2019) and the Botportal database (http://botbioger.versailles.inra.fr/botportal/; Simon & Viaud, 2018) were used for the manual curation of cytochrome P450s, taurine catabolism dioxygenases, cutinases, sugar transporters, sedolisins, serine carboxypeptidases and metallopeptidases. Functional categories with significant enrichment were identified using Fisher's exact test with a p-value cutoff at 0.05 (only the Bcin genes analyzed by the chip were used for this test).

Expression profiling by quantitative PCR analysis

Experiments were performed as described by Rascle *et al*. (2018). RT-qPCR experiments were performed using ABI-7900 Applied Biosystems (Applied Biosystems). Amplification reactions were carried out using SYBR Green PCR Master Mix (Applied Biosystems). Relative quantification was based on the $2(-\Delta\Delta C(T))$ method (Livak & Schmittgen, 2001) using the *BcactA* (Bcin16g02020), *Bcef1α* gene (Bcin09g05760), and *Bcpda1* gene (Bcin07g01890) as normalization internal controls. At least three independent biological replicates were analyzed. Primers used for RT-qPCR are shown in Table S5.

ROS and melanin production

For visualization of melanin, a stock solution of the DHN melanogenesis inhibitor tricyclazole (Sigma) was prepared in acetone (10 mg ml^{-1}). Three-day-old 2-mm mycelial plugs were deposited in 6-well plates. Droplets (50 µl) of PDB¼ (supplemented or not with 50 µg ml^{-1} tricyclazole) medium were added on the plugs. After 48 h incubation (21°C), IC were observed by reverse microscopy. For visualization of ROS produced during IC formation, 100 µl of medium were added to 1 ml of DAB (Sigma) solution (0.05% in 100 mM citric acid buffer pH 3.7) and

incubated 20 h in darkness with gentle agitation. Controls were done by adding 1 µl Horse Radish Peroxydase (HRP - Thermoscientific) to 1 ml DAB in presence of different quantities of H_2O_2.

Quantitative proteomic analysis

The steps of sample preparation and protein digestion were performed as previously described (Dieryckx *et al.*, 2015) and online nanoLC-MS/MS analyses were performed using an Ultimate 3000 RSLC Nano-UPHLC system (Thermo Scientific) coupled to a nanospray Q Exactive hybrid quadrupole-Orbitrap mass spectrometer (Thermo Scientific). The parameters of the LC-MS method used were as previously described (Pineda *et al.*, 2018). Protein identification and Label-Free Quantification (LFQ) were done in Proteome Discoverer 2.3. MS Amanda 2.0, Sequest HT and Mascot 2.4 algorithms were used for protein identification in batch mode by searching against the Ensembl *Botrytis cinerea* B05.10 database (ASM83294v1, 13 749 entries, release 98.3). Two missed enzyme cleavages were allowed. Mass tolerances in MS and MS/MS were set to 10 ppm and 0.02 Da. Oxidation (M), acetylation (K) and deamidation (N, Q) were searched as dynamic modifications and carbamidomethylation (C) as static modification. Peptide validation was performed using Percolator algorithm (Käll *et al.*, 2007) and only "high confidence" peptides were retained, corresponding to a 1% false discovery rate at peptide level. Minora feature detector node (LFQ) was used along with the feature mapper and precursor ions quantifier. The normalization parameters were selected as follows: (1) Unique peptides, (2) Precursor abundance based on intensity, (3) Normalization mode: total peptide amount, (4) Protein abundance calculation: summed abundances, (5) Protein ratio calculation: pairwise ratio based and (6) Hypothesis test: t-test (background based). Quantitative data were considered for master proteins, quantified by a minimum of 2 unique peptides, a fold change ≥3 and a statistical p-value lower than 0.05. The mass spectrometry proteomics data have been deposited

to the ProteomeXchange Consortium (http://proteomecentral.proteomexchange.org) via the PRIDE partner repository (Perez-Riverol *et al*., 2019) with the dataset identifier PXD016885.

Construction of deletion mutants in *Botrytis cinerea*

Δ*Bcflp1* and Δ*Bcflp2* deletion mutants were constructed using a gene replacement strategy (Fig.S5). The replacement cassettes were generated by combining double-joint PCR (Yu *et al*., 2004) and split-marker approach (Catlett *et al.*, 2003). All primers are listed in Table S4. The three gene replacement cassettes were verified by sequencing. *B. cinerea* transformation was carried out using protoplasts as previously described by Rascle *et al.* (2018), except that the protoplasts were transformed with 1µg of each split-marker cassette DNA and plated on medium containing 200 $g.l^{-1}$ saccharose and 2 $g.l^{-1}$ $NaNO_3$ supplemented with 70 $\mu g.ml^{-1}$ hygromycin (Invivogen, France) for single Δ*Bcflp1* or Δ*Bcflp2* mutants or 80 $\mu g.ml^{-1}$ nourseothricin (Werner BioAgents, Germany) for double replacement mutants. Diagnostic PCR was performed to detect homologous recombination in the selected resistant transformants. Homokaryotic transformants were obtained after several rounds of single-spore isolation. Southern blot analyses were performed to ensure single insertions. Genomic DNA digested with *Eco*RI was hybridized with the 3'- flanking region of *Bcflp1* (amplified with Probe1For and Probe1Rev primers) or the 5'-flanking region of *Bcflp2* (amplified with Probe2For and Probe2Rev primers) using the PCR DIG Probe Synthesis Kit and the DIG Luminescent Detection Kit (Roche, Germany) following manufacturer's instructions.

Pathogenicity tests

Infection assays were performed with one-week-old French bean (*Phaseolus vulgaris* var *Saxa*) leaves using 4-mm 72-h-old mycelial plugs from *B. cinerea* WT, Δ*Bcflp1*, Δ*Bcflp2* and Δ*Bcflp1*::Δ*Bcflp2* mutant strains grown on sporulation medium. Infected plants were incubated at 21°C under 100% relative humidity and dark (10 h)-daylight (14 h) conditions. Necrosis zone

diameter was measured daily. All tests were assessed in three independent experiments, with at least eight plants and thirty points of infection for each strain.

Microscopy

Confocal microscopy and imaging were performed with a Zeiss LSM510 confocal microscope (Oberkochen, Germany) and its integrated ZEN software. For staining of chitin and chitosan, the fungal culture medium was drained and replaced by 1 ml H_2O containing 20 µl KOH 10%, 10 µl Calcofluor (Fluka, 1g/L) and 10 µl eosin Y 0.5% (Sigma). Following 10 min incubation in the dark, the staining solution was drained, the samples were washed 5 times with 1 ml H_2O and overlaid with 0.5 ml H_2O. Fluorescent signals of calcofluor and eosin Y were respectively captured using a 405 nm and 561 nm excitation wavelength.

Acknowledgements

We thank Adeline Simon, Lucile Albinet and Luna Nadjare for providing tools and help on bioinformatic analyses. We thank Gwenlyn Fleury for her implication in the study of fasclicin mutants, and Cindy Dieryckx and Vincent Girard for their advices on secretome analysis. We are thankful to Glen Calvar for English editing.

Conflict of Interest

The authors have no conflict of interest to declare.

References

Akutsu, K., Kobayashi, Y., Matsuzawa, Y., Watanabe, T., Ko, K., and Misato, T. (1981) Morphological studies on infection process of cucumber leaves by conidia of *Botrytis cinerea* stimulated with various purine-related compounds. *Japanese Journal of Phytopathology* **47**: 234–243.

Almagro Armenteros, J.J., Tsirigos, K.D., Sønderby, C.K., Petersen, T.N., Winther, O., Brunak, S., et al. (2019) SignalP 5.0 improves signal peptide predictions using deep neural networks. *Nature Biotechnology* **37**: 420–423.

Amselem, J., Cuomo, C.A., van Kan, J.A.L., Viaud, M., Benito, E.P., Couloux, A., et al. (2011) Genomic Analysis of the Necrotrophic Fungal Pathogens *Sclerotinia sclerotiorum* and *Botrytis cinerea*. *PLoS Genetics* **7**: e1002230.

An, B., Li, B., Li, H., Zhang, Z., Qin, G., and Tian, S. (2016) Aquaporin8 regulates cellular development and reactive oxygen species production, a critical component of virulence in *Botrytis cinerea*. *New Phytologist* **209**: 1668–1680.

Backhouse, D. and Willetts, H.J. (1987) Development and structure of infection cushions of *Botrytis cinerea*. *Transactions of the British Mycological Society* **89**: 89–95.

Baker, L.G., Specht, C.A., Donlin, M.J., and Lodge, J.K. (2007) Chitosan, the Deacetylated Form of Chitin, Is Necessary for Cell Wall Integrity in *Cryptococcus neoformans*. *Eukaryot Cell* **6**: 855.

Billon-Grand, G., Rascle, C., Droux, M., Rollins, J.A., and Poussereau, N. (2012) pH modulation differs during sunflower cotyledon colonization by the two closely related necrotrophic fungi *Botrytis cinerea* and *Sclerotinia sclerotiorum*: *Botrytis* and *Sclerotinia* differ in pH modulation. *Molecular Plant Pathology* **13**: 568–578.

Blanco-Ulate, B., Morales-Cruz, A., Amrine, K.C.H., Labavitch, J.M., Powell, A.L.T., and Cantu, D. (2014) Genome-wide transcriptional profiling of *Botrytis cinerea* genes targeting plant cell walls during infections of different hosts. *Frontiers in plant science* **5**: 435.

Boenisch, M.J. and Schäfer, W. (2011) *Fusarium graminearum* forms mycotoxin producing infection structures on wheat. *BMC Plant Biology* **11**: 110.

Brito, N., Espino, J.J., and González, C. (2006) The Endo-β-1,4-Xylanase Xyn11A Is Required for Virulence in *Botrytis cinerea*. *MPMI* **19**: 25–32.

Catlett, N.L., Lee, B.-N., Yoder, O.C., and Turgeon, B.G. (2003) Split-Marker Recombination for Efficient Targeted Deletion of Fungal Genes. *Fungal Genetics Reports* **50**: 9–11.

Choquer, M., Fournier, E., Kunz, C., Levis, C., Pradier, J.-M., Simon, A., and Viaud, M. (2007) *Botrytis cinerea* virulence factors: new insights into a necrotrophic and polyphageous pathogen. *FEMS Microbiology Letters* **277**: 1–10.

Chrissian, C., Camacho, E., Fu, M.S., Prados-Rosales, R., Chatterjee, S., Cordero, R.J.B., et al. (2020) Melanin deposition in two *Cryptococcus* species depends on cell-wall composition and flexibility. *Journal of Biological Chemistry* **295**: 1815–1828.

Cohrs, K.C., Simon, A., Viaud, M., and Schumacher, J. (2016) Light governs asexual differentiation in the grey mould fungus *Botrytis cinerea* via the putative transcription factor BcLTF2: BcLTF2 regulates conidiation in *Botrytis cinerea*. *Environmental Microbiology* **18**: 4068–4086.

Collado, I.G. and Viaud, M. (2016) Secondary Metabolism in *Botrytis cinerea*: Combining Genomic and Metabolomic Approaches. In *Botrytis – the Fungus, the Pathogen and its Management in Agricultural Systems*. Fillinger, S. and Elad, Y. (eds). Cham: Springer International Publishing, pp. 291–313.

Cord-Landwehr, S., Melcher, R.L.J., Kolkenbrock, S., and Moerschbacher, B.M. (2016) A chitin deacetylase from the endophytic fungus *Pestalotiopsis sp*. efficiently inactivates the elicitor activity of chitin oligomers in rice cells. *Scientific Reports* **6**: 38018.

Cuesta Arenas, Y., Kalkman, E.R.I.C., Schouten, A., Dieho, M., Vredenbregt, P., Uwumukiza, B., et al. (2010) Functional analysis and mode of action of phytotoxic Nep1-like proteins of *Botrytis cinerea*. *Physiological and Molecular Plant Pathology* **74**: 376–386.

Cutler, H.G., Jacyno, J.M., Harwood, J.S., Dulik, D., Goodrich, P.D., and Roberts, R.G. (1993) Botcinolide: A Biologically Active Natural Product from *Botrytis cinerea*. *Bioscience, Biotechnology, and Biochemistry* **57**: 1980–1982.

Cutler, H.G., Parker, S.R., Ross, S.A., Crumley, F.G., and Schreiner, P.R. (1996) Homobotcinolide: A Biologically Active Natural Homolog of Botcinolide from *Botrytis cinerea*. *Bioscience, Biotechnology, and Biochemistry* **60**: 656–658.

Dalmais, B., Schumacher, J., Moraga, J., Le Pêcheur, P., Tudzynski, B., Collado, I.G., and Viaud, M. (2011) The *Botrytis cinerea* phytotoxin botcinic acid requires two polyketide synthases for production and has a redundant role in virulence with botrydial: Botcinic acid biosynthesis gene clusters. *Molecular Plant Pathology* **12**: 564–579.

Daniels, A., Lucas, J.A., and Peberdy, J.F. (1991) Morphology and ultrastructure of W and R pathotypes of *Pseudocercosporella herpotrichoides* on wheat seedlings. *Mycological Research* **95**: 385–397.

De Vallée, A., Bally, P., Bruel, C., Chandat, L., Choquer, M., Dieryckx, C., et al. (2019) A Similar Secretome Disturbance as a Hallmark of Non-pathogenic *Botrytis cinerea* ATMT-Mutants? *Front Microbiol* **10**: 2829.

Dean, R., Van Kan, J.A.L., Pretorius, Z.A., Hammond-Kosack, K.E., Di Pietro, A., Spanu, P.D., et al. (2012) The Top 10 fungal pathogens in molecular plant pathology. *Molecular Plant Pathology* **13**: 414–430.

Deighton, N., Muckenschnabel, I., Colmenares, A.J., Collado, I.G., and Williamson, B. (2001) Botrydial is produced in plant tissues infected by *Botrytis cinerea*. *Phytochemistry* **57**: 689–692.

Deising, H.B., Werner, S., and Wernitz, M. (2000) The role of fungal appressoriain plant infection. *Microbes and Infection* **2**: 1631–1641.

Demirci, E. and Döken, M.T. (1998) Host Penetration and Infection by the Anastomosis Groups of *Rhizoctonia solani Kühn* Isolated from Potatoes. *Turkish Journal of Agriculture and Forestry* **22**: 609–613.

Dieryckx, C., Gaudin, V., Dupuy, J.-W., Bonneu, M., Girard, V., and Job, D. (2015) Beyond plant defense: insights on the potential of salicylic and methylsalicylic acid to contain growth of the phytopathogen *Botrytis cinerea*. *Frontiers in Plant Science* **6**: 859.

Dinh, S.Q., Joyce, D.C., Irving, D.E., and Wearing, A.H. (2011) Histology of waxflower (*Chamelaucium spp*.) flower infection by *Botrytis cinerea*. *Plant Pathology* **60**: 278–287.

Elad, Y., Pertot, I., Prado, A.M.C., and Stewart, A. (2016) Plant hosts of *Botrytis spp*. In *Botrytis–the fungus, the pathogen and its management in agricultural systems*. Springer, pp. 413–486.

Emmett, R.W. and Parbery, D.G. (1975) Appressoria. *Annual Review of Phytopathology* **13**: 147–165.

Espino, J.J., Brito, N., Noda, J., and González, C. (2005) *Botrytis cinerea* endo-ß-1,4-glucanase Cel5A is expressed during infection but is not required for pathogenesis. *Physiological and Molecular Plant Pathology* **66**: 213–221.

Fogarty, R.V. and Tobin, J.M. (1996) Fungal melanins and their interactions with metals. *Enzyme and Microbial Technology* **19**: 311–317.

Fourie, J.F. and Holz, G. (1994) Infection of plum and nectarine flowers by *Botrytis cinerea*. *Plant Pathology* **43**: 309–315.

Franzen, A.J., Cunha, M.M.L., Batista, E.J.O., Seabra, S.H., De Souza, W., and Rozental, S. (2006) Effects of tricyclazole (5-methyl-1,2,4-triazol[3,4] benzothiazole), a specific DHN–melanin inhibitor, on the morphology of *Fonsecaea pedrosoi* conidia and sclerotic cells. *Microscopy Research and Technique* **69**: 729–737.

Frías, M., Brito, N., and González, C. (2013) The *Botrytis cinerea* cerato-platanin BcSpl1 is a potent inducer of systemic acquired resistance (SAR) in tobacco and generates a wave of salicylic acid expanding from the site of application. *Molecular Plant Pathology* **14**: 191–196.

Frías, M., González, M., González, C., and Brito, N. (2016) BcIEB1, a *Botrytis cinerea* secreted protein, elicits a defense response in plants. *Plant Science* **250**: 115–124.

Fullerton, R.A., Harris, F.M., and Hallett, I.C. (1999) Rind distortion of lemon caused by *Botrytis cinerea* Pers. *New Zealand Journal of Crop and Horticultural Science* **27**: 205–214.

García, N., González, M.A., González, C., and Brito, N. (2017) Simultaneous Silencing of Xylanase Genes in *Botrytis cinerea*. *Frontiers in Plant Science* **8**: 2174.

Garcia-Arenal, F. and Sagasta, E.M. (1980) Scanning electron microscopy of *Botrytis cinerea* penetration of bean (*Phaseolus vulgaris*) hypocotyls. *Phytopathologische Zeitschrift* **99**: 37–42.

Geoghegan, I.A. and Gurr, S.J. (2016) Chitosan mediates germling adhesion in *Magnaporthe oryzae* and is required for surface sensing and germling morphogenesis. *PLoS Pathogens* **126**: e1005703.

Gladders, P. and Coley-Smith, J.R. (1977) Infection cushion formation in *Rhizoctonia tuliparum*. *Transactions of the British Mycological Society* **68**: 115–118.

Glass, N.L., Schmoll, M., Cate, J.H.D., and Coradetti, S. (2013) Plant Cell Wall Deconstruction by Ascomycete Fungi. *Annual Review of Microbiology* **67**: 477–498.

Gonzalez, C., Brito, N., and Sharon, A. (2016) Infection Process and Fungal Virulence Factors. In *Botrytis - The Fungus, the Pathogen and its Management in Agricultural Systems*. pp. 229–246.

Govrin, E.M. and Levine, A. (2000) The hypersensitive response facilitates plant infection by the necrotrophic pathogen *Botrytis cinerea*. *Current Biology* **10**: 751–757.

Govrin, E.M., Rachmilevitch, S., Tiwari, B.S., Solomon, M., and Levine, A. (2006) An Elicitor from *Botrytis cinerea* Induces the Hypersensitive Response in *Arabidopsis thaliana* and Other Plants and Promotes the Gray Mold Disease. *Phytopathology* **96**: 299–307.

Hao, F., Ding, T., Wu, M., Zhang, J., Yang, L., Chen, W., and Li, G. (2018) Two Novel Hypovirulence-Associated Mycoviruses in the Phytopathogenic Fungus *Botrytis cinerea*: Molecular Characterization and Suppression of Infection Cushion Formation. *Viruses* **10**: 254.

Hou, J., Feng, H., Chang, H., Liu, Y., Li, G., Yang, S., et al. (2020) The H3K4 demethylase Jar1 orchestrates ROS production and expression of pathogenesis-related genes to facilitate *Botrytis cinerea* virulence. *New Phytologist* **225**: 930–947.

Käll, L., Canterbury, J.D., Weston, J., Noble, W.S., and MacCoss, M.J. (2007) Semi-supervised learning for peptide identification from shotgun proteomics datasets. *Nature Methods* **4**: 923–925.

Kars, I., Krooshof, G.H., Wagemakers, L., Joosten, R., Benen, J.A.E., and Kan, J.A.L.V. (2005) Necrotizing activity of five *Botrytis cinerea* endopolygalacturonases produced in *Pichia pastoris*. *The Plant Journal* **43**: 213–225.

Kelloniemi, J., Trouvelot, S., Héloir, M.-C., Simon, A., Dalmais, B., Frettinger, P., et al. (2015) Analysis of the Molecular Dialogue Between Gray Mold (*Botrytis cinerea*) and

Grapevine (*Vitis vinifera*) Reveals a Clear Shift in Defense Mechanisms During Berry Ripening. *Mol Plant Microbe Interact* **28**: 1167–1180.
Kong, W., Chen, N., Liu, T., Zhu, J., Wang, J., He, X., and Jin, Y. (2015) Large-Scale Transcriptome Analysis of Cucumber and *Botrytis cinerea* during Infection. *PLoS One* **10**: e0142221–e0142221.
Kuroki, M., Okauchi, K., Yoshida, S., Ohno, Y., Murata, S., Nakajima, Y., et al. (2017) Chitin-deacetylase activity induces appressorium differentiation in the rice blast fungus *Magnaporthe oryzae*. *Scientific Reports* **7**: 9697.
Lam, W.C., Upadhya, R., Specht, C.A., Ragsdale, A.E., Hole, C.R., Levitz, S.M., and Lodge, J.K. (2019) Chitosan Biosynthesis and Virulence in the Human Fungal Pathogen *Cryptococcus gattii*. *mSphere* **4**: e00644-19.
Li, Y., Han, Y., Qu, M., Chen, J., Chen, X., Geng, X., et al. (2020) Apoplastic Cell Death-Inducing Proteins of Filamentous Plant Pathogens: Roles in Plant-Pathogen Interactions. *Front. Genet.* **11**:661.
Liu, J.-K., Chang, H.-W., Liu, Y., Qin, Y.H., Ding, Y.-H., Wang, L., et al. (2018) The key gluconeogenic gene *PCK1* is crucial for virulence of *Botrytis cinerea* via initiating its conidial germination and host penetration: Gluconeogenesis regulates *B. cinerea* pathogenesis. *Environmental Microbiology* **20**: 1794–1814.
Liu, T., Chen, G., Min, H., and Lin, F. (2009) MoFLP1, encoding a novel fungal fasciclin-like protein, is involved in conidiation and pathogenicity in *Magnaporthe oryzae*. *J Zhejiang Univ Sci B* **10**: 434–444.
Liu, Z., Gay, L.M., Tuveng, T.R., Agger, J.W., Westereng, B., Mathiesen, G., et al. (2017) Structure and function of a broad-specificity chitin deacetylase from *Aspergillus nidulans* FGSC A4. *Scientific Reports* **7**: 1746.
Livak, K.J. and Schmittgen, T.D. (2001) Analysis of Relative Gene Expression Data Using Real-Time Quantitative PCR and the $2^{-\Delta\Delta CT}$ Method. *Methods* **25**: 402–408.
Lombard, V., Golaconda Ramulu, H., Drula, E., Coutinho, P.M., and Henrissat, B. (2014) The carbohydrate-active enzymes database (CAZy) in 2013. *Nucleic Acids Research* **42**: D490–D495.
Lumsden, R.D. and Wergin, W.P. (1980) Scanning-Electron Microscopy of Infection of Bean by Species of *Sclerotinia*. *Mycologia* **72**: 1200–1209.
Mani, I., Sharma, V., Tamboli, I., and Raman, G. (2001) Interaction of Melanin with Proteins – The Importance of an Acidic Intramelanosomal pH. *Pigment Cell Research* **14**: 170–179.
Marschall, R. and Tudzynski, P. (2016a) BcIqg1, a fungal IQGAP homolog, interacts with NADPH oxidase, MAP kinase and calcium signaling proteins and regulates virulence and development in *Botrytis cinerea*: BcIqg1-a central scaffold protein in *Botrytis cinerea*. *Molecular Microbiology* **101**: 281–298.
Marschall, R. and Tudzynski, P. (2016b) Reactive oxygen species in development and infection processes. *Seminars in Cell & Developmental Biology* **57**: 138–146.
Marschall, R. and Tudzynski, P. (2017) The Protein Disulfide Isomerase of *Botrytis cinerea*: An ER Protein Involved in Protein Folding and Redox Homeostasis Influences NADPH Oxidase Signaling Processes. *Frontiers in Microbiology* **8**: 960.
Massaroli, M., Moraga, J., Bastos Borges, K., Ramírez-Fernández, J., Viaud, M., González Collado, I., et al. (2013) A Shared Biosynthetic Pathway for Botcinins and Botrylactones Revealed through Gene Deletions. *ChemBioChem* **14**: 132–136.
Mentges, M., Glasenapp, A., Boenisch, M., Malz, S., Henrissat, B., Frandsen, R.J.N., et al. (2020) Infection cushions of *Fusarium graminearum* are fungal arsenals for wheat infection. *Molecular Plant Pathology*. 00:1–18.

Michielse, C.B., Becker, M., Heller, J., Moraga, J., Collado, I.G., and Tudzynski, P. (2011) The *Botrytis cinerea* Reg1 Protein, a Putative Transcriptional Regulator, Is Required for Pathogenicity, Conidiogenesis, and the Production of Secondary Metabolites. *Molecular Plant-Microbe Interactions*® **24**: 1074–1085.

Mitchell, A.L., Attwood, T.K., Babbitt, P.C., Blum, M., Bork, P., Bridge, A., et al. (2018) InterPro in 2019: improving coverage, classification and access to protein sequence annotations. *Nucleic Acids Research* **47**: D351–D360.

Nafisi, M., Stranne, M., Zhang, L., van Kan, J.A.L., and Sakuragi, Y. (2014) The Endo-Arabinanase BcAra1 Is a Novel Host-Specific Virulence Factor of the Necrotic Fungal Phytopathogen *Botrytis cinerea*. *Molecular Plant-Microbe Interactions*® **27**: 781–792.

Nie, J., Yin, Z., Li, Z., Wu, Y., and Huang, L. (2019) A small cysteine-rich protein from two kingdoms of microbes is recognized as a novel pathogen-associated molecular pattern. *New Phytologist* **222**: 995-1011.

Noda, J., Brito, N., and González, C. (2010) The *Botrytis cinerea* xylanase Xyn11A contributes to virulence with its necrotizing activity, not with its catalytic activity. *BMC Plant Biol* **10**: 38.

O'Connell, R., Thon, M., Hacquard, S., Amyotte, S.G., Kleemann, J., Torres, M.F., et al. (2012) Lifestyle transitions in plant pathogenic *Colletotrichum* fungi deciphered by genome and transcriptome analyses. *Nature Genetics* **44,** 1060–1065.

Patel, P.K. and Free, S.J. (2019) The Genetics and Biochemistry of Cell Wall Structure and Synthesis in *Neurospora crassa*, a Model Filamentous Fungus. *Frontiers in Microbiology* **10**: 2294.

Pepin, R. (1980) Le comportement parasitaire de *Sclerotinia tuberosa (hedw.) Fuckel* sur *Anemone nemorosa L*. Etude en microscopie photonique et électronique a balayage. *Mycopathologia* **72**: 89–99.

Perez-Dulzaides, R., Camacho, E., Cordero, R.J.B., and Casadevall, A. (2018) Cell-wall dyes interfere with *Cryptococcus neoformans* melanin deposition. *Microbiology* **164**: 1012–1022.

Pérez-Hernández, A., González, M., González, C., van Kan, J.A.L., and Brito, N. (2017) BcSUN1, a *B. cinerea* SUN-Family Protein, Is Involved in Virulence. *Front Microbiol* **8**: 35.

Perez-Riverol, Y., Csordas, A., Bai, J., Bernal-Llinares, M., Hewapathirana, S., Kundu, D.J., et al. (2018) The PRIDE database and related tools and resources in 2019: improving support for quantification data. *Nucleic Acids Research* **47**: D442–D450.

Pineda, E., Thonnus, M., Mazet, M., Mourier, A., Cahoreau, E., Kulyk, H., et al. (2018) Glycerol supports growth of the *Trypanosoma brucei* bloodstream forms in the absence of glucose: Analysis of metabolic adaptations on glycerol-rich conditions. *PLoS Pathog* **14**: e1007412.

Pinedo, C., Moraga, J., Barua, J., González-Rodríguez, V.E., Aleu, J., Durán-Patrón, R., et al. (2016) Chemically Induced Cryptic Sesquiterpenoids and Expression of Sesquiterpene Cyclases in *Botrytis cinerea* Revealed New Sporogenic (+)-4- *Epi* eremophil-9-en-11-ols. *ACS Chemical Biology* **11**: 1391–1400.

Porquier, A., Moraga, J., Morgant, G., Dalmais, B., Simon, A., Sghyer, H., et al. (2019) Botcinic acid biosynthesis in *Botrytis cinerea* relies on a subtelomeric gene cluster surrounded by relics of transposons and is regulated by the Zn2Cys6 transcription factor BcBoa13. *Current Genetics* **65**: 965–980.

Priebe, S., Kreisel, C., Horn, F., Guthke, R., and Linde, J. (2015) FungiFun2: a comprehensive online resource for systematic analysis of gene lists from fungal species. *Bioinformatics* **31**: 445–446.

Prior, G. and Owen, J. (1964) Pathological anatomy of *Sclerotinia trifoliorum* on clover and alfalfa. *Phytopathology* **54**: 784–787.
Qutob, D., Kemmerling, B., Brunner, F., Küfner, I., Engelhardt, S., Gust, A.A., et al. (2006) Phytotoxicity and innate immune responses induced by Nep1-like proteins. *The Plant Cell* **18**: 3721–3744.
R Core Team (2019) R: A Language and Environment for Statistical Computing, Vienna, Austria: R Foundation for Statistical Computing.
Rascle, C., Dieryckx, C., Dupuy, J.W., Muszkieta, L., Souibgui, E., Droux, M., et al. (2018) The pH regulator PacC: a host-dependent virulence factor in *Botrytis cinerea*. *Environ Microbiol Rep* **10**: 555–568.
Rheinländer, P.A., Sutherland, P.W., and Fullerton, R.A. (2013) Fruit infection and disease cycle of *Botrytis cinerea* causing cosmetic scarring in persimmon fruit (Diospyros kaki Linn.). *Australasian Plant Pathology* **42**: 551–560.
Rolke, Y., Liu, S., Quidde, T., Williamson, B., Schouten, A., Weltring, K.-M., et al. (2004) Functional analysis of H2O2-generating systems in *Botrytis cinerea*: the major Cu-Zn-superoxide dismutase (BCSOD1) contributes to virulence on French bean, whereas a glucose oxidase (BCGOD1) is dispensable. *Molecular Plant Pathology* **5**: 17–27.
Rossi, F.R., Gárriz, A., Marina, M., Romero, F.M., Gonzalez, M.E., Collado, I.G., and Pieckenstain, F.L. (2011) The Sesquiterpene Botrydial Produced by *Botrytis cinerea* Induces the Hypersensitive Response on Plant Tissues and Its Action Is Modulated by Salicylic Acid and Jasmonic Acid Signaling. *Molecular Plant-Microbe Interactions®* **24**: 888–896.
Ryder, L.S. and Talbot, N.J. (2015) Regulation of appressorium development in pathogenic fungi. *Current Opinion in Plant Biology* **26**: 8–13.
Sapmak, A., Boyce, K.J., Andrianopoulos, A., and Vanittanakom, N. (2015) The pbrB gene encodes a laccase required for DHN-melanin synthesis in conidia of *Talaromyces (Penicillium) marneffei*. *PloS one* **10**: e0122728.
Schouten, A., Baarlen, P.V., and Kan, J.A.L.V. (2008) Phytotoxic Nep1-like proteins from the necrotrophic fungus *Botrytis cinerea* associate with membranes and the nucleus of plant cells. *New Phytologist* **177**: 493–505.
Schumacher, J. (2016) DHN melanin biosynthesis in the plant pathogenic fungus *Botrytis cinerea* is based on two developmentally regulated key enzyme (PKS)-encoding genes: DHN melanogenesis in *Botrytis cinerea*. *Molecular Microbiology* **99**: 729–748.
Segmüller, N., Kokkelink, L., Giesbert, S., Odinius, D., van Kan, J., and Tudzynski, P. (2008) NADPH Oxidases Are Involved in Differentiation and Pathogenicity in *Botrytis cinerea*. *MPMI* **21**: 808–819.
Seifert, G. (2018) Fascinating Fasciclins: A Surprisingly Widespread Family of Proteins that Mediate Interactions between the Cell Exterior and the Cell Surface. *International Journal of Molecular Sciences* **19**: 1628.
Sharman, S. and Heale, J.B. (1977) Penetration of carrot roots by the grey mould fungus *Botrytis cinerea* Pers. ex Pers. *Physiological Plant Pathology* **10**: 63–71.
Shlezinger, N., Minz, A., Gur, Y., Hatam, I., Dagdas, Y.F., Talbot, N.J., and Sharon, A. (2011) Anti-Apoptotic Machinery Protects the Necrotrophic Fungus *Botrytis cinerea* from Host-Induced Apoptotic-Like Cell Death during Plant Infection. *PLOS Pathogens* **7**: e1002185.
Siegmund, U. and Viefhues, A. (2016) Reactive Oxygen Species in the *Botrytis* – Host Interaction. In *Botrytis – the Fungus, the Pathogen and its Management in Agricultural Systems*. Fillinger, S. and Elad, Y. (eds). Cham: Springer International Publishing, pp. 269–289.

Simon, A. and Biot, E. (2010) ANAIS: Analysis of NimbleGen Arrays Interface. *Bioinformatics* **26**: 2468–2469.
Simon, A. and Viaud, M. (2018) Cross-reference table for Botrytis cinerea B0510 and T4 gene ids. https://doi.org/10.15454/IHYJCX, Portail Data INRAE, V2, UNF:6:PgcjbcKsoy-oUHnNO6LX9Vg== [fileUNF]
Smith, V., Punja, Z., and Jenkins, S. (1986) A histological study of infection of host tissue by *Sclerotium rolfsii*. *Phytopathology* **76**: 755–759.
Soanes, D.M., Chakrabarti, A., Paszkiewicz, K.H., Dawe, A.L. and Talbot, N.J. (2012) Genome-wide transcriptional profiling of appressorium development by the rice blast fungus *Magnaporthe oryzae*. *PLoS Pathogens* **8**: e1002514.Stewart, A., Backhouse, D., Sutherland, P.W., and Fullerton, R.A. (1989) The Development of Infection Structures of *Sclerotium cepivorum* on Onion. *Journal of Phytopathology* **126**: 22–32.
Sun, L.-L., Li, M., Suo, F., Liu, X.-M., Shen, E.-Z., Yang, B., et al. (2013) Global analysis of fission yeast mating genes reveals new autophagy factors. *PLoS Genet* **9**: e1003715.
Tariq, V.N. and Jeffries, P. (1984) Appressorium formation by *Sclerotinia sclerotiorum*: Scanning electron microscopy. *Transactions of the British Mycological Society* **82**: 645–651.
Ten Have, A., Espino, J.J., Dekkers, E., Van Sluyter, S.C., Brito, N., Kay, J., et al. (2010) The *Botrytis cinerea* aspartic proteinase family. *Fungal Genetics and Biology* **47**: 53–65.
Upadhya, R., Baker, L.G., Lam, W.C., Specht, C.A., Donlin, M.J., and Lodge, J.K. (2018) *Cryptococcus neoformans* Cda1 and Its Chitin Deacetylase Activity Are Required for Fungal Pathogenesis. *mBio* **9**: e02087-18.
Van den Brink, J. and de Vries, R.P. (2011) Fungal enzyme sets for plant polysaccharide degradation. *Appl Microbiol Biotechnol* **91**: 1477–1492.
Van den Heuvel, J. and Waterreus, L.P. (1983) Conidial concentration as an important factor determining the type of prepenetration structures formed by *Botrytis cinerea* on leaves of French bean (*Phaseolus vulgaris*). *Plant Pathology* **32**: 263–272.
Van Kan, J.A.L., Stassen, J.H.M., Mosbach, A., Van Der Lee, T.A.J., Faino, L., Farmer, A.D., et al. (2017) A gapless genome sequence of the fungus *Botrytis cinerea*: Gapless Genome Sequence of *B. cinerea*. *Molecular Plant Pathology* **18**: 75–89.
Viefhues, A., Heller, J., Temme, N., and Tudzynski, P. (2014) Redox Systems in *Botrytis cinerea* : Impact on Development and Virulence. *Molecular Plant-Microbe Interactions®* **27**: 858–874.
Viefhues, A., Schlathoelter, I., Simon, A., Viaud, M., and Tudzynski, P. (2015) Unraveling the Function of the Response Regulator BcSkn7 in the Stress Signaling Network of *Botrytis cinerea*. *Eukaryot Cell* **14**: 636.
Vu, V.V., Beeson, W.T., Span, E.A., Farquhar, E.R., and Marletta, M.A. (2014) A family of starch-active polysaccharide monooxygenases. *Proceedings of the National Academy of Sciences* **111**: 13822–13827.
Xie, M., Zhao, X., Lü, Y., and Jin, C. (2020) Chitin deacetylases Cod4 and Cod7 are involved in polar growth of *Aspergillus fumigatus*. *Microbiologyopen* **9**: e00943–e00943.
Yu, J.-H., Hamari, Z., Han, K.-H., Seo, J.-A., Reyes-Domínguez, Y., and Scazzocchio, C. (2004) Double-joint PCR: a PCR-based molecular tool for gene manipulations in filamentous fungi. *Fungal Genet Biol* **41**: 973–981.
Zhang, L., De Wu, M., Li, G.Q., Jiang, D.H., and Huang, H.C. (2010) Effect of Mitovirus infection on formation of infection cushions and virulence of *Botrytis cinerea*. *Physiological and Molecular Plant Pathology* **75**: 71–80.
Zhang, M.-Z., Sun, C.-H., Liu, Y., Feng, H.-Q., Chang, H.-W., Cao, S.-N., et al. (2020) Transcriptome analysis and functional validation reveal a novel gene, BcCGF1, that enhances fungal virulence by promoting infection-related development and host penetration. *Molecular Plant Pathology* **21**: 834–853.

938 Zhang, W., Corwin, J.A., Copeland, D.H., Feusier, J., Eshbaugh, R., Cook, D.E., et al. (2019)
939 Plant–necrotroph co-transcriptome networks illuminate a metabolic battlefield. *eLife* **8**:
940 e44279.
941 Zhang, Yi, Zhang, Yunhua, Qiu, D., Zeng, H., Guo, L., and Yang, X. (2015) BcGs1, a glyco-
942 protein from *Botrytis cinerea*, elicits defence response and improves disease resistance
943 in host plants. *Biochemical and biophysical research communications* **457**: 627–634.
944 Zhu, W., Ronen, M., Gur, Y., Minz-Dub, A., Masrati, G., Ben-Tal, N., et al. (2017) BcXYG1,
945 a Secreted Xyloglucanase from *Botrytis cinerea,* Triggers Both Cell Death and Plant
946 Immune Responses. *Plant Physiol* **175**:438-456.

Functional subcategories (expert annotation manually curated)	**Correspondence with the GO (Biological Process)**	**Proposed biological roles**	**Up-regulated genes** (**1231**/11134)	**Enrichment p-value**	**Sources used for curation**
1: PCWDE*_Cellulose (C)	Carbohydrate metabolic process	Plant degradation Nutrition	**5**/19	>5E-2	CAZy database (Lombard *et al*., 2013); www.cazy.org/ Van den Brink & de Vries (2011) ; Glass (2013)
2: PCWDE*_Hemicellulose (H)			**17**/32	**5.6E-9**	
3: PCWDE*_Pectin (P)			**18**/48	**1.6E-6**	
4: PCWDE*_C_H_P			**13**/26	**9.1E-7**	
5: FCWE**_Chitin deacetylases (CDA)		Fungal cell wall remodeling	**3**/5	**1.2E-2**	Liu *et al.* (2017)
6: Alpha-1,2-mannosidases		unknown	**4**/5	**6.8E-4**	GH92 family in CAZy database
7: ROS producing systems	Oxidation-reduction process	ROS	**14**/54	**1.8E-3**	Siegmund and Viefhues (2016) ; Botportal database
8: ROS detoxification and scavenging			**7**/41	>5E-2	
9: Cytochrome P450s		Phytotoxins, others	**26**/128	**2.5E-3**	IPR001128***
10: Botcinic acid biosynthesis genes (Boa)		Phytotoxins	**10**/10	**2.7E-10**	Porquier *et al*., 2019
11: Botrydial biosynthesis genes (Bot)			**7**/7	**5.6E-8**	Dalmais *et al*., 2011
12: Taurine catabolism dioxygenase TauD/TfdA		unknown	**4**/14	>5E-2	IPR003819***
13: Secondary metabolism key enzyme genes (e.g. PKS, NRPS, TS, DMATS)****	Metabolic process	Phytotoxins, ROS, others	**11**/42	**4.9E-3**	Collado and Viaud (2016)
14: DHN-melanogenic genes		Fungal cell wall remodeling	**6**/11	**5.1E-4**	Schumacher (2016); Cohrs *et al.* (2016)
15: Cutinases		Plant degradation	**4**/11	**2.6E-2**	IPR000675***
16: Sugar transporters	Transmembrane transport	Nutrition	**22**/86	**1.7E-4**	IPR003663; IPR005829; IPR007271; IPR004689***
17: Aspartyl Proteases	Proteolysis	Plant degradation Nutrition	**6**/14	**2.5E-3**	ten Have *et al*. (2010)
18: Sedolisins			**5**/10	**2.6E-3**	IPR030400***
19: Serine carboxypeptidases			**4**/16	>5E-2	IPR001563, IPR008758, IPR001375***
20: Metallopeptidases			**4**/10	**1.9E-2**	IPR024079***
21: Putative secreted proteins (signalP)	All categories	Virulence	**266**/1079	**8.0E-41**	SignalP-5.0 (Almagro Armenteros *et al*., 2019)
22: Plant Cell Death-Inducing Proteins (CDIP)			**6**/14	**2.5E-3**	Liu *et al.* (2020)

Table 1: Functional enrichment analysis of up-regulated genes in the infection cushion of *Botrytis cinerea*.

Functional category	Subcategory (expert annotation)	Description	Protein ID	Name	FC	p-value	Sources used for curation
Metabolic process	Plant cuticle degradation	Cutinase (CE5)	Bcin15p00130		54	2,2E-12	IPR000675***
			Bcin08p01580		15	1,2E-06	
Carbohydrate and polysaccharide metabolic processes	PCWDE* - Cellulose	Endo-beta-1,4-glucanase (GH5_5)	Bcin03p04010	BcCel5A	4	7,3E-03	Espino *et al.* (2005)
	PCWDE* - Hemicellulose	**Xylanase (GH11) (CDIP)**	**Bcin03p00480**	**BcXyn11A**	**40**	**7,1E-11**	**Brito *et al.* (2006)**
		Xylanase (GH10,CBM1)	Bcin05p06020	BcXyn10B	5	4,3E-03	Garcia *et al.* (2017)
		Xylosidase (GH31)	Bcin11p06440		3	2,8E-02	CAZy DB****
	PCWDE* - Cellulose and Hemicellulose	**Xyloglucanase (GH12) (CDIP)**	**Bcin03p03630**	**BcXyg1**	**54**	**2,0E-12**	**Zhu *et al.* (2017)**
		Xyloglucanase (GH12 CBM1)	Bcin13p02320		53	2,3E-12	CAZy DB****
	PCWDE* - Pectin	Rhamnogalacturonan acetylesterase (CE12)	Bcin02p07100		8	1,5E-04	
		Pectin methyl esterase (CE8)	Bcin01p11150		1000	9,0E-17	
			Bcin08p02970	BcPme1	13	4,6E-06	Kars *et al.* (2005)
	Starch degradation (nutrition)	**Glucoamylase (GH15, CBM20) (CDIP)**	**Bcin04p04190**	**BcGs1**	**164**	**9,0E-17**	Zhang *et al.*, 2015
		Glucoamylase (GH15)	Bcin04p00030		19	1,7E-07	CAZy DB****
		Alpha amylase (GH13)	Bcin02p01420		94	2,0E-15	
		Lytic starch monooxygenase (AA13, CBM20)	Bcin06p05050		33	5,4E-10	Vu *et al.* (2014)
	FCWE** remodeling - polysaccharides crosslinking	Beta-1,3-Glucan transferase GAS (GH72)	Bcin02p06940	BcGas1	5	3,0E-03	Patel and Free (2019) CAZy DB****
			Bcin13p02330		3	2,7E-02	
			Bcin14p03970		3	2,8E-02	
		Beta-1,3-Glucan transferase BGL2 (GH17)	Bcin09p00200		15	1,2E-06	
			Bcin01p11220		5	6,1E-03	
		Alpha-1,6-mannanase Dfg5/Dcw1 (GH76)	Bcin08p06110		14	2,3E-06	
		Chitin / Glucan transglycosylase CRH (GH16)	Bcin01p06010		8	1,9E-04	
	PCWDE* or FCWE** Glucan hydrolysis	Beta Glucanase (GH131)	Bcin12p06120		8	2,4E-04	CAZy DB****
		Beta Glucanase (GH131, CBM1)	Bcin09p01150		7	3,2E-04	
		Beta-1,3-Glucanase (GH55)	Bcin10p00310		3	4,6E-02	
	Other fungal cell wall proteins	WSC domain protein	Bcin15p00810		100	9,0E-17	IPR002889***
		LysM effector (CBM50) - chitin binding	Bcin02p05630	BcLysM1	28	4,2E-09	Crumière *et al.* (unpublished)
	Unknown	Non classified Glycosyl Hydrolase (GHnc)	Bcin04p01310		6	1,9E-03	CAZy DB****
		Putative expansin (CBM63)	Bcin01p02460		5	4,3E-03	

Table 2: Up-accumulated proteins in the secretome from the infection cushion of *Botrytis cinerea*. (1/3)

Functional category	Subcategory (expert annotation)	Description	Protein ID	Name	FC	p-value	Sources used for curation
	Proteolysis	Aspartic protease	Bcin12p02040	BcAp8	656	9,0E-17	Ten Have *et al.* (2010)
			Bcin05p05900	BcAp5	25	9,9E-09	
			Bcin12p00180	BcAp9	19	1,8E-07	
			Bcin04p02060	BcAp13	4	1,2E-02	
		Sedolisin	Bcin08p01020		1000	9,0E-17	IPR030400***
			Bcin15p03150		172	9,0E-17	
			Bcin15p04670	BcSer8	44	2,1E-11	
			Bcin06p00620	BcTpp2	22	4,1E-08	
			Bcin06p00330		18	3,2E-07	
			Bcin10p01890		12	1,0E-05	
		Serine carboxypeptidase	Bcin08p00280		269	9,0E-17	IPR001563*** IPR008758*** IPR001375***
			Bcin08p02390		10	3,7E-05	
			Bcin06p02510		8	2,0E-04	
		Metallopeptidase	Bcin16p02770	BcMp1	276	9,0E-17	IPR024079***
		Glutamic protease	Bcin15p02380	BcAcp1	997	9,0E-17	Billon-Grand *et al.* (2012)
		Putative peptidase S41	Bcin07p04370		48	8,6E-12	
Oxidation-reduction process	ROS producing systems	Glucose-methanol-choline oxidoreductase	Bcin03p01540		53	2,7E-12	Siegmund and Viefhues (2016) Botportal DB Simon & Viaud (2018)
			Bcin02p07080		16	6,3E-07	
			Bcin12p02910		7	7,2E-04	
		Laccase	Bcin14p02510	BcLcc2	1000	9,0E-17	
			Bcin01p00800	BcLcc8	6	1,2E-03	
	ROS detoxification and scavenging	Dyp-type peroxidase	Bcin13p05720	BcPrd1	1000	9,0E-17	
		Peroxidase	Bcin03p07850	BcPrd10	26	8,0E-09	
	Other oxydases	Glyoxal oxidase 2 (AA5)	Bcin12p01520	BcGo2	1000	9,0E-17	Botportal DB Simon & Viaud (2018)
		Putative oxidase	Bcin02p00280		18	3,0E-07	
			Bcin02p00220		12	9,5E-06	
			Bcin05p00580		12	1,2E-05	
			Bcin03p00380		4	1,7E-02	

Table 2: Up-accumulated proteins in the secretome from the infection cushion of *Botrytis cinerea*. (2/3)

Functional category	Subcategory (expert annotation)	Description	Protein ID	Name	FC	p-value	Sources used for curation
Other or unknown functions	Nucleases	S1/P1 Nuclease	Bcin07p06590		81	1,2E-14	Botportal DB Simon & Viaud (2018)
		Ribonuclease T2	Bcin03p07320		73	4,2E-14	
			Bcin04p03620		3	3,3E-02	
	Phosphatases	Acid phosphatase	Bcin15p03320		15	1,2E-06	
		Phytase subfamily of histidine acid phosphatase	Bcin07p04290	BcHap1	7	4,8E-04	
	Esterases	Carboxylesterase	Bcin16p02130		8	1,9E-04	
		Putative esterase	Bcin02p08230		7	6,0E-04	
	Other enzymes	Carboxymuconate cyclase	Bcin12p03690		9	1,0E-04	
		Glutamate dehydrogenase	Bcin16p04050		5	5,6E-03	
	Other proteins	**Necrosis & ethylene-inducing protein (CDIP)**	**Bcin02p07770**	**BcNep2**	**137**	**9,0E-17**	Schouten *et al.* (2008)
		Glycoprotein necrosis inducer (CDIP)	**Bcin15p00100**	**BcIeb1**	**112**	**9,0E-17**	Frias *et al.* (2016)
		Cerato-platanin family protein (CDIP)	**Bcin03p00500**	**BcSpl1**	**78**	**1,7E-14**	Frias *et al.* (2013)
		Ubiquitin 3 binding protein But2	Bcin09p05250		40	6,4E-11	Botportal DB
		Putative Ferritin	Bcin16p03990		18	3,0E-07	
		Fasciclin-like protein	Bcin04p05020	BcFlp1	16	8,8E-07	This study
	Hypothetical proteins		Bcin14p00810		1000	9,0E-17	
			Bcin06p06670		34	5,0E-10	
			Bcin09p02890		19	1,6E-07	
			Bcin01p06060		18	3,5E-07	
			Bcin11p02610		5	3,8E-03	
			Bcin09p00220		4	7,5E-03	
			Bcin12p00750		3	3,3E-02	

Table 2: Up-accumulated proteins in the secretome from the infection cushion of *Botrytis cinerea*. (3/3)

Table 1: Functional enrichment analysis of up-regulated genes in the infection cushion of *Botrytis cinerea*.

Functional subcategories were determined according to a GO biological process analysis followed by a manual curation using existing databases and published data. Categories with significant enrichment were identified using Fisher's exact test with a p-value cutoff at 0.05 (only the Bcin genes analyzed by the chip were used for this test); Number of differentially regulated genes (in bold) and p-values are indicated. *PCWDE, Plant Cell Wall Degrading Enzymes; **FCWE, Fungus Cell Wall Enzymes; *** Bcin proteins displaying an "IPR" InterPro domain (www.ebi.ac.uk/interpro/; Mitchell *et al.*, 2019) were searched on the Botportal database (http://botbioger.versailles.inra.fr/botportal/; Simon & Viaud, 2018); **** PKS, Polyketide synthases; NRPS, Non-Ribosomal Peptide Synthetases; TS, Terpen cyclases; DMATS, Dimethylallyl tryptophan synthases.

Table 2: Up-accumulated proteins in the secretome from the infection cushion of *Botrytis cinerea*.

Comparison of IC secretome versus mycelium secretome revealed 79 proteins up-accumulated. For quantification, all unique peptides of an identified protein were included, and the total cumulative abundance was calculated by summing the abundances of all peptides allocated to the respective protein. ANOVA test was applied at the protein level. Three independent biological experiments were conducted and analyzed. The mass spectrometry proteomics data have been deposited to the ProteomeXchange Consortium via the PRIDE partner repository with the dataset identifier PXD016885. Gene ID and protein accession numbers can be found in Ensembl Fungi release database (http://fungi.ensembl.org/Botrytis_cinerea/Info/Index). The fold change values (FC) between the average protein abundances in the IC and the vegetative mycelia are indicated with the associated p-values. The up-accumulated proteins, identified in 3 biological

replicates with a minimum of 2 unique peptides, are listed and classified according to their functional category (manual annotation). *PCWDE, Plant Cell Wall Degrading Enzymes according to Van den Brink & de Vries (2011) and Glass (2013); **FCWE, Fungus Cell Wall Enzymes; *** Bcin proteins displaying an "IPR" InterPro domain (www.ebi.ac.uk/interpro/; Mitchell et al., 2019) were searched on the Botportal database (http://botbioger.versailles.inra.fr/botportal/; Simon & Viaud, 2018); **** CAZy database (Lombard *et al.*, 2014 ; www.cazy.org/). Six plant cell death-inducing proteins (CDIP; Li *et al.*, 2020) are shown in bold. (Additional information is provided in Table S3).

Figure legends

Figure 1: Scanning Electron Microscopy of *Botrytis cinerea* infection cushion.

Mature infection cushion, produced on glass surface, developing multiple and successive ramifications of hyphae (2 dpi).

Figure 2: Up-regulation of phytotoxins and ROS production in the infection cushion of *Botrytis cinerea*

(a) Hierarchical clustering of the expression of the Botcinic acid genes (*Bcboa)* and botrydial genes (*Bcbot)* in infection cushion. (IC, 4 biological replicates) and control mycelium (Myc, 3 biological replicates). The normalized expression intensities are clustered and represented by color-coded squares; Shades of green and red depict down- and up-regulation in IC, respectively (fold change (FC) $\leq$ -2 or $\geq$ 2 and FDR<0.05). (b) Botcinic acid (boa) and botrydial (bot) structures (left; Pinedo *et al*., 2016) and biosynthesis gene clusters (right; Porquier *et al*., 2019 and Dalmais *et al*., 2011). Genes up-regulated in IC are colored in red. Genes with no chip reference and whose expression could hence not be measured are colored in white. (c) Visualization of ROS produced by IC. 100 µl of medium were added to 1ml of DAB and incubated

20h. Controls were done by adding 1µl Horse Radish Peroxydase (HRP) to 1ml DAB in presence of different quantities of H_2O_2. The growth medium of 48 h cellophane-overlaid liquid cultures (IC) or agitated liquid cultures (Myc) was mixed to a DAB solution. The oxidation of DAB by H_2O_2 in the presence of peroxidases is revealed by a brown coloration.

Figure 3: Regulation of the DHN melanogenesis bipartite pathway in the infection cushion of *Botrytis cinerea.*

This figure is adapted from Schumacher *et al*. (2016) and Cohrs *et al*. (2016). (a) Hierarchical clustering of the expression of DHN-melanogenic genes in IC (IC, 4 replicates) and control mycelium (Myc, 3 replicates) as presented in figure 2. Up-regulated genes that co-localize with the DHN-melanogenic genes are added for information (*), but their role in melanin biosynthesis remains to be established. Similarly, 2 laccases up-regulated genes (*Bclcc6* and *Bclcc8*) are listed (**), but their role in melanin biosynthesis remains to be established. (b) DHN-melanins biosynthesis putative gene clusters. (c) DHN-melanin metabolic pathway and targets of tricyclazole (lightnings). Genes up- or down-regulated in IC and corresponding proteins are colored in red and green, respectively. (d) Light microscopy images of hyphae and IC of *B. cinerea* produced on plastic surface in the absence (top) and presence (bottom) of tricyclazole. Pigmented IC versus hyaline hyphae (left) and dark versus orange-brown thick cell walls inside IC (right) are shown. Bars represent 10 µm.

Figure 4: Cell wall chitin deacetylation in the infection cushion of *Botrytis cinerea*.

(a) Representation of the transformation of chitin into chitosan by chitin deacetylases (cda). (b) Hierarchical clustering of the expression of 5 putative *cda* genes in infection cushion (IC) and control mycelium (Myc), as presented in figure 2. (c) Expression of *Bccda* genes during a kinetics of bean leaves infection by *B. cinerea* (dpi; days post inoculation). Expression levels

were calculated following the $2^{-\Delta\Delta CT}$ method using constitutively expressed actin gene *BcactA* (Bcin16g02020) as a reference. The use of two other housekeeping genes, elongation factor *Bcef1α* (Bcin09g05760) and pyruvate dehydrogenase *Bcpda1* (Bcin07g01890) gave similar results (data not shown). Three independent biological replicates were assessed for each experiment. Standard errors are displayed, and asterisks indicate a significant difference in gene expression compared with the previous time point (Student's *t* test, * p-value <0.05). (d) Confocal microscopy of mycelium and mature IC produced onto a plastic surface at 44 hpi and double-stained with Calcofluor targeting mainly chitin (blue) and Eosin Y targeting mainly chitosan (yellow).

Figure 5: *In planta* RT-qPCR validation of microarray up-regulated genes.

(a) and (b) Infection cushions development on leaves infected by *B. cinerea*. Primary bean leaves were inoculated with conidia and fungal development (1-4 days post inoculation (dpi)) was monitored using a Stereomicroscope (Zeiss) and cotton blue to stain the fungal cells at the plant surface. IC are pointed by white arrows. Bars represent 5 mm (a) or 50 µm (b). (c) Expression of selected genes during infection. Infected bean leaves were collected to prepare RNAs and RT-qPCR was used to measure the expression of 14 genes up-regulated in IC produced *in vitro* conditions (microarray data) and whose predicted function relates to virulence. The red bar indicates the peak of expression for each gene (when 2 or 3 bars are in red for the same gene, statistics cannot distinguish them). Gene expression levels were calculated following the $2^{-\Delta\Delta CT}$ method using constitutively expressed actin gene *BcactA* (Bcin16g02020) as a reference. The use of two other housekeeping genes, elongation factor *Bcef1α* (Bcin09g05760) and pyruvate dehydrogenase *Bcpda1* (Bcin07g01890) showed similar results (data not shown). Standard errors of three independent biological replicates are displayed and asterisks indicate a

significant difference in gene expression compared with the previous time point (Student's *t* test, p-value <0.05).

Figure 6: Characterization of fasciclin-like deletion mutants in *Botrytis cinerea*.

(a) Infection kinetics - French bean leaves were inoculated with mycelial plugs of the WT and deletion strains. The necrosis of the plant tissues was measured every 24 h (at least eight plants and 32 infection points) over 4 days in 3 independent experiments. Bars indicate standard errors. (b) Visualization of the necrotic lesions. At 72 h post inoculation, typical images of bean leaves infected by the WT and mutant strains are presented. White arrows indicate dark rings at the edge of the necrotic zones. (c) Growth *in vitro*: The WT strain, the single mutant strains (Δ*Bcflp1* and Δ*Bcflp2*) and the double mutant strain (Δ*Bcflp1*::Δ*Bcflp2*) were grown on minimal medium for 72h. The diameters of the colonies were measured on 4 independent experiments conducted with 5 plates for each strain. Bars indicate standard errors and stars indicate significant differences (Student *t*-test, p-value <0.05) between the WT and the mutants. Similar results were recorded for all experiments on two independent strains of each mutant.

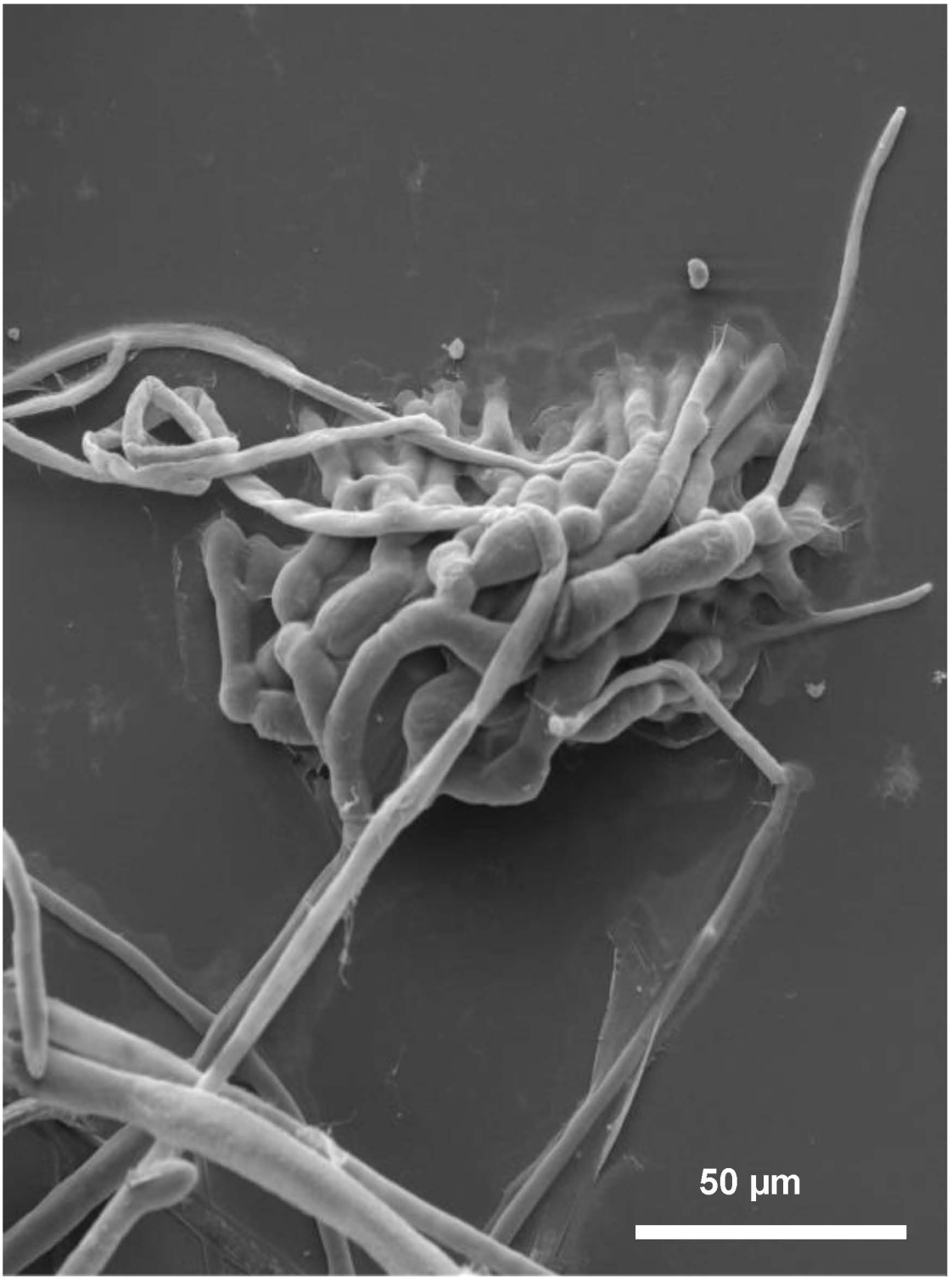
50 µm

Figure 2

a

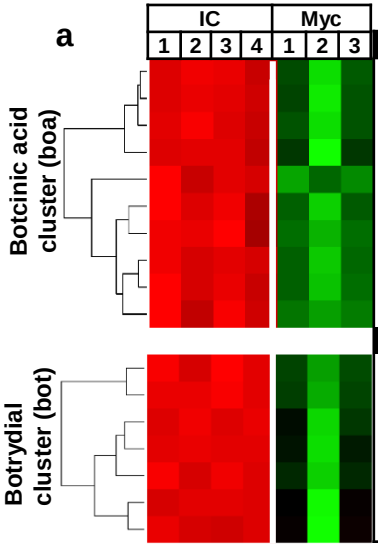

Gene ID	Chip reference	FC	FDR	Name	Description
Bcin01g00020	BC1G_16083	24	3.8^{E}-3	*Bcboa2*	Monooxygenase
Bcin01g00030	BC1G_16084	15	4.8^{E}-3	*Bcboa3*	Cytochrome P450
Bcin01g00120	BC1G_15842	12	3.6^{E}-4	*Bcboa12*	Unknown function
Bcin01g00090	BC1G_15837	6.6	1.1^{E}-2	*Bcboa9*	Polyketide synthase (PKS9)
Bcin01g00080	BC1G_15836	10	7.4^{E}-4	*Bcboa8*	FAD-binding domain
Bcin01g00110	BC1G_15841	31	3.3^{E}-3	*Bcboa11*	3-o-acetyltransferase
Bcin01g00100	BC1G_15840	17	2.0^{E}-3	*Bcboa10*	Thioesterase
Bcin01g00040	BC1G_16085	30	1.9^{E}-3	*Bcboa4*	Cytochrome P450
Bcin01g00060	BC1G_16087	12	1.6^{E}-3	*Bcboa6*	Polyketide synthase (PKS6)
Bcin01g00130	BC1G_15843	35	7.7^{E}-4	*Bcboa13*	Transcription factor
Bcin12g06370	BCexp5_BCL4	3.1	1.7^{E}-3	*Bcbot4*	P450 monooxygenase
Bcin12g06410	BCexp1_BCL5	7.5	2.2^{E}-3	*Bcbot5*	Acetyl transferase
Bcin12g06430	BofuT4_P065690	2.4	8.9^{E}-3	*Bcbot7*	Dehydrogenase
Bcin12g06400	BCexp2_CND11	4.3	1.2^{E}-2	*Bcbot3*	P450 monooxygenase
Bcin12g06420	BofuT4_P065700	10	6.8^{E}-3	*Bcbot6*	$Zn(II)_2Cys_6$ transcription factor
Bcin12g06390	BCexp3_CND15	4.2	2.7^{E}-2	*Bcbot2*	Sesquiterpene cyclase (STC1)
Bcin12g06380	BCexp4_CND5	2.0	3.4^{E}-2	*Bcbot1*	P450 monooxygenase

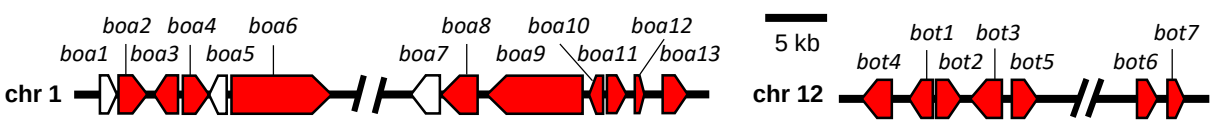

b

DAB	+	+	+	+	+	+	+
HRP	-	-	-	+	+	+	+
H_2O_2 (%)	-	-	-	3^{E-4}	6^{E-4}	3^{E-3}	3^{E-2}
Growth medium	+	+	-	-	-	-	-

Figure 3

a

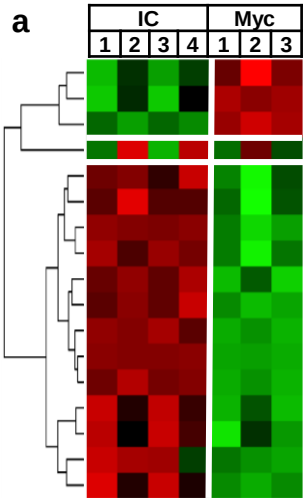

Gene ID	Chip reference	FC	FDR	Name	Description
Bcin02g08760	BofuT4_P088390	-2.1	2.2^{E}-2	*Bcsmr1*	Transcription factor
Bcin15g01680	BofuT4_P005890	-2.8	3.0^{E}-2	*Bcscd2*	Scytalone dehydratase
Bcin02g08770	BofuT4_P088370	-4.2	1.4^{E}-3	*Bcpks12*	Polyketide synthase
Bcin03g08080	BofuT4_P077260	1.1	7.8^{E}-1	*Bcztf2*	Transcription factor
Bcin03g08090	BofuT4_P077280	1.96	1.9^{E}-2	*Bcztf1*	Transcription factor
Bcin04g04790	BofuT4_P094400	**2.1**	**2.7^{E}-2**	No	Methyl transferase (*)
Bcin04g04780	BofuT4_P094420	**2.1**	**1.4^{E}-3**	No	Unknown function (*)
Bcin15g03330	BofuT4_P003560	**15**	**6.6^{E}-3**	*Bclcc6*	Laccase (**)
Bcin03g08120	BofuT4_P077310	**6.0**	**4.8^{E}-3**	No	Monooxygenase (*)
Bcin02g04370	BofuT4_P122670	**2.8**	**3.1^{E}-3**	No	Unknown function (*)
Bcin03g08110	BofuT4_P077300	**5.6**	**1.1^{E}-3**	*Bcscd1*	Scytalone dehydratase
Bcin04g04800	BofuT4_P094390	**53**	**5.1^{E}-5**	*Bcbrn1*	THN reductase
Bcin02g04360	BofuT4_P122660	**3.1**	**1.1^{E}-3**	*Bcygh1*	Hydrolase
Bcin03g08050	BofuT4_P077210	**5.0**	**2.4^{E}-2**	*Bcpks13*	Polyketide synthase
Bcin16g02090	BofuT4_P033780	**5.4**	**4.4^{E}-2**	*Bcltf2*	Transcription factor
Bcin03g08100	BofuT4_P077290	**3.7**	**4.5^{E}-2**	*Bcbrn2*	THN reductase
Bcin01g00800	BofuT4_P154790	**3.0**	**2.8^{E}-2**	*Bclcc8*	Laccase (**)

b

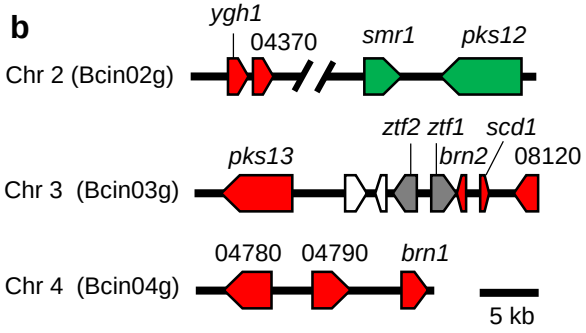

c

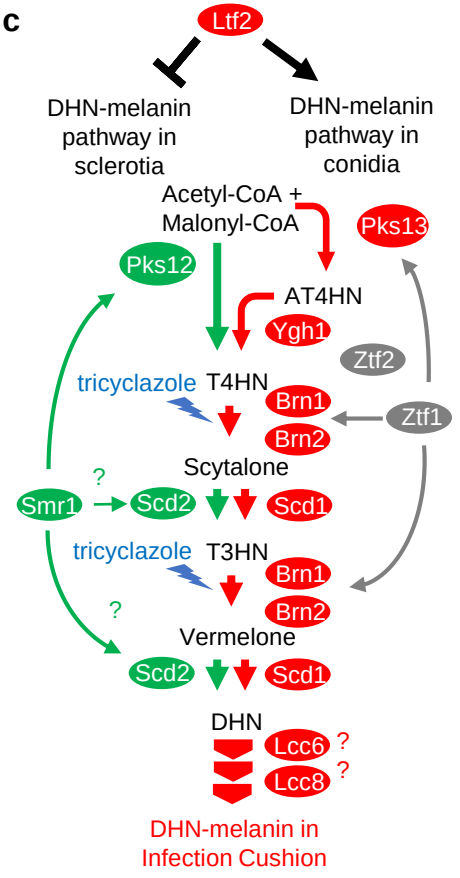

d

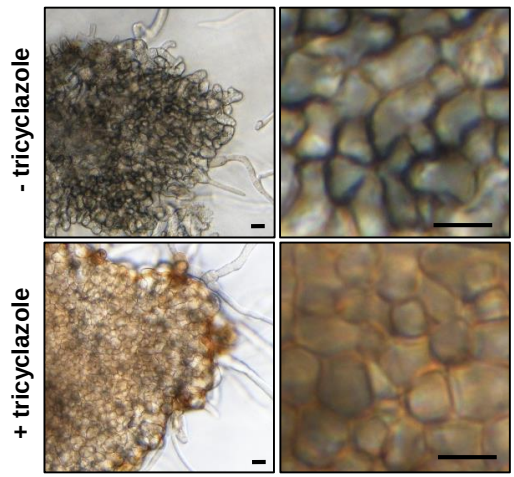

Figure 4

a

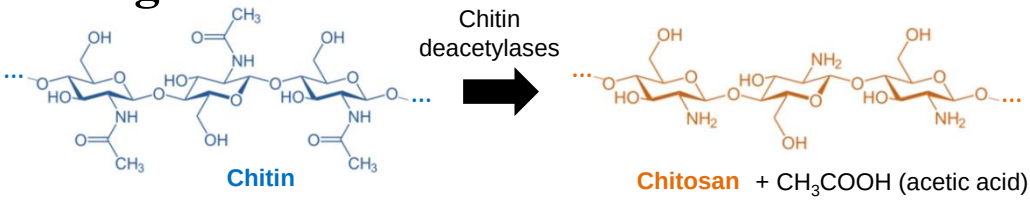

b

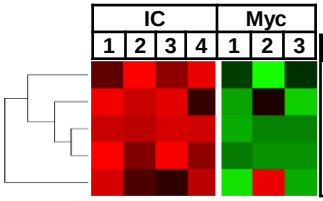

Gene ID	Chip reference	FC	FDR	Name
Bcin09g00620	BofuT4_P101030	**4.1**	**2.9^{E}-2**	***Bccda4***
Bcin11g04800	BofuT4_P079220	1.7	3.9^{E}-2	*Bccda2*
Bcin03g02970	BofuT4_P051770	**18**	**3.6^{E}-4**	***Bccda3***
Bcin03g05710	BofuT4_P018380	**55**	**4.1^{E}-3**	***Bccda1***
Bcin01g08990	BofuT4_P050320	1.2	3.3^{E}-1	*Bccda5*

c

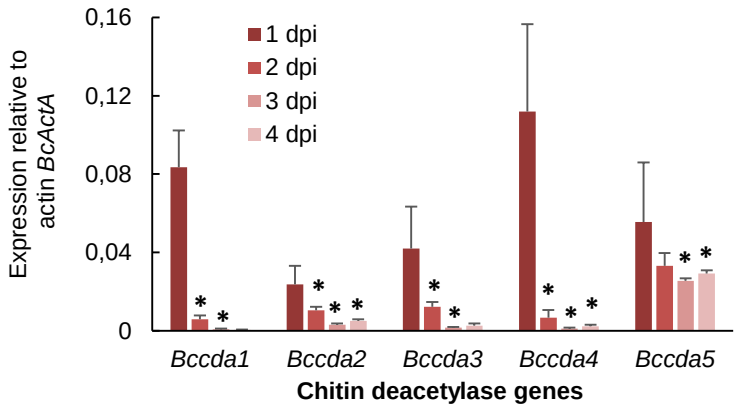

d

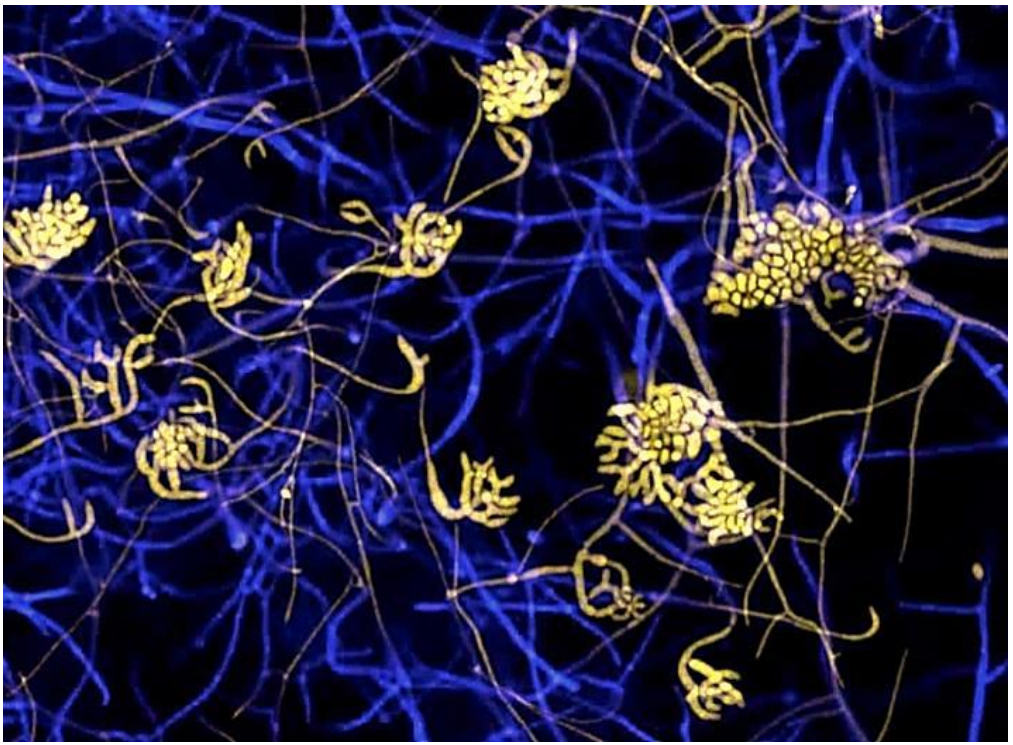

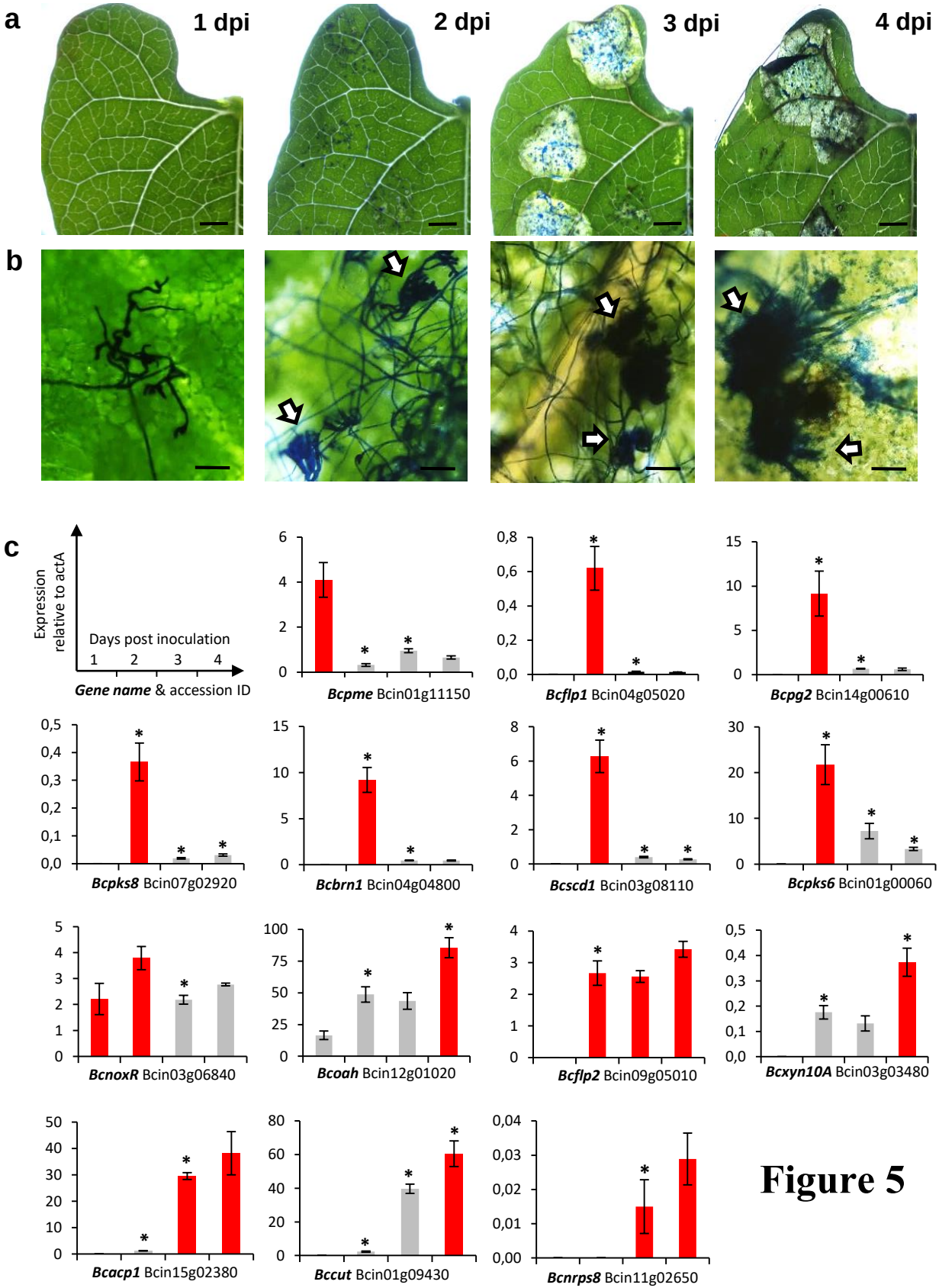
a
1 dpi
2 dpi
3 dpi
4 dpi
b
c
Expression relative to actA
Days post inoculation
1 2 3 4
Gene name & accession ID
Bcpme Bcin01g11150
Bcflp1 Bcin04g05020
Bcpg2 Bcin14g00610
Bcpks8 Bcin07g02920
Bcbrn1 Bcin04g04800
Bcscd1 Bcin03g08110
Bcpks6 Bcin01g00060
BcnoxR Bcin03g06840
Bcoah Bcin12g01020
Bcflp2 Bcin09g05010
Bcxyn10A Bcin03g03480
Bcacp1 Bcin15g02380
Bccut Bcin01g09430
Bcnrps8 Bcin11g02650

Figure 5

Figure 6

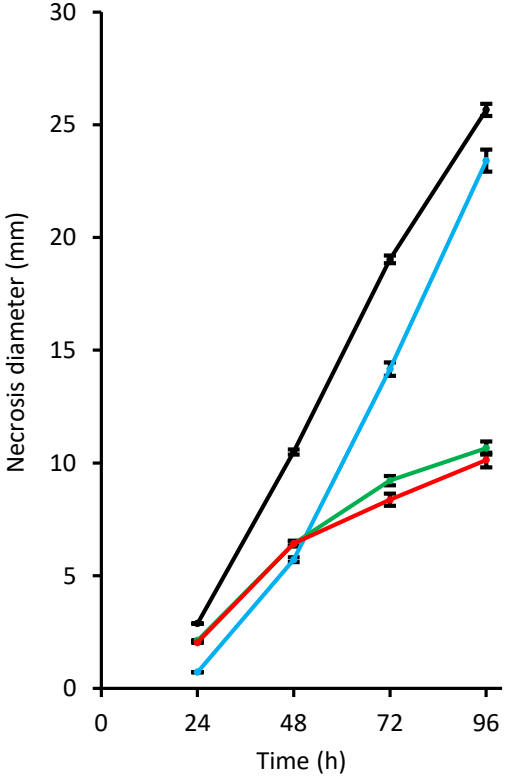
a
30
25
20
15
10
5
0
Necrosis diameter (mm)
0
24
48
72
96
Time (h)

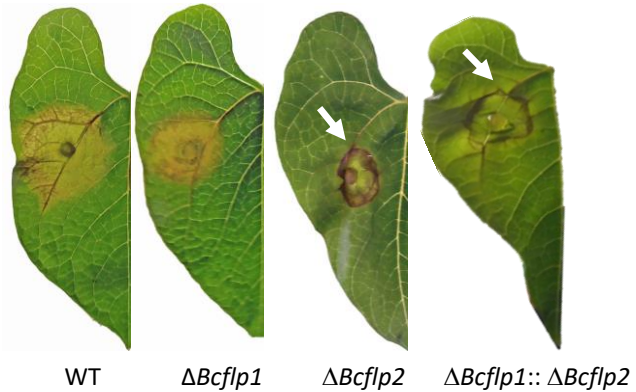
b
WT
ΔBcflp1
ΔBcflp2
ΔBcflp1:: ΔBcflp2

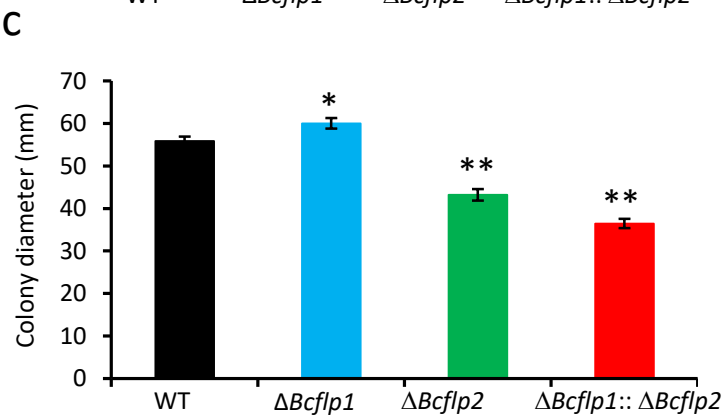
c
70
60
50
40
30
20
10
0
Colony diameter (mm)
*
**
**
WT
ΔBcflp1
ΔBcflp2
ΔBcflp1:: ΔBcflp2

Supporting Information

Article title: **The infection cushion of *Botrytis cinerea*: a fungal "weapon" of plant-biomass destruction**
Authors: Mathias Choquer, Christine Rascle, Isabelle R Gonçalves, Amélie de Vallée, Cécile Ribot, Elise Loisel, Pavlé Smilevski, Jordan Ferria, Mahamadi Savadogo, Eytham Souibgui, Marie-Josèphe Gagey, Jean-William Dupuy, Jeffrey A Rollins, Riccardo Marcato, Camille Noûs, Christophe Bruel and Nathalie Poussereau

The following Supporting Information is available for this article:

Fig. S1 *In vitro* production of infection cushions of *Botrytis cinerea*. (a) Light microscopy of mycelia produced from conidia of *B. cinerea* spread onto PDA plates overlaid with cellophane and culture for 44h. Mature and melanized infection cushions (dark patchs) were fully differentiated and hyperbranched and they covered about 40% of the PDA plates surfaces (b) Light microscopy of mycelia produced from conidia inoculated in PDB-containing flasks and cultured under agitation for 44h. The liquid cultures produced only mycelium and no infection cushion. Magnifications are indicated.

Supplementary Figure S1

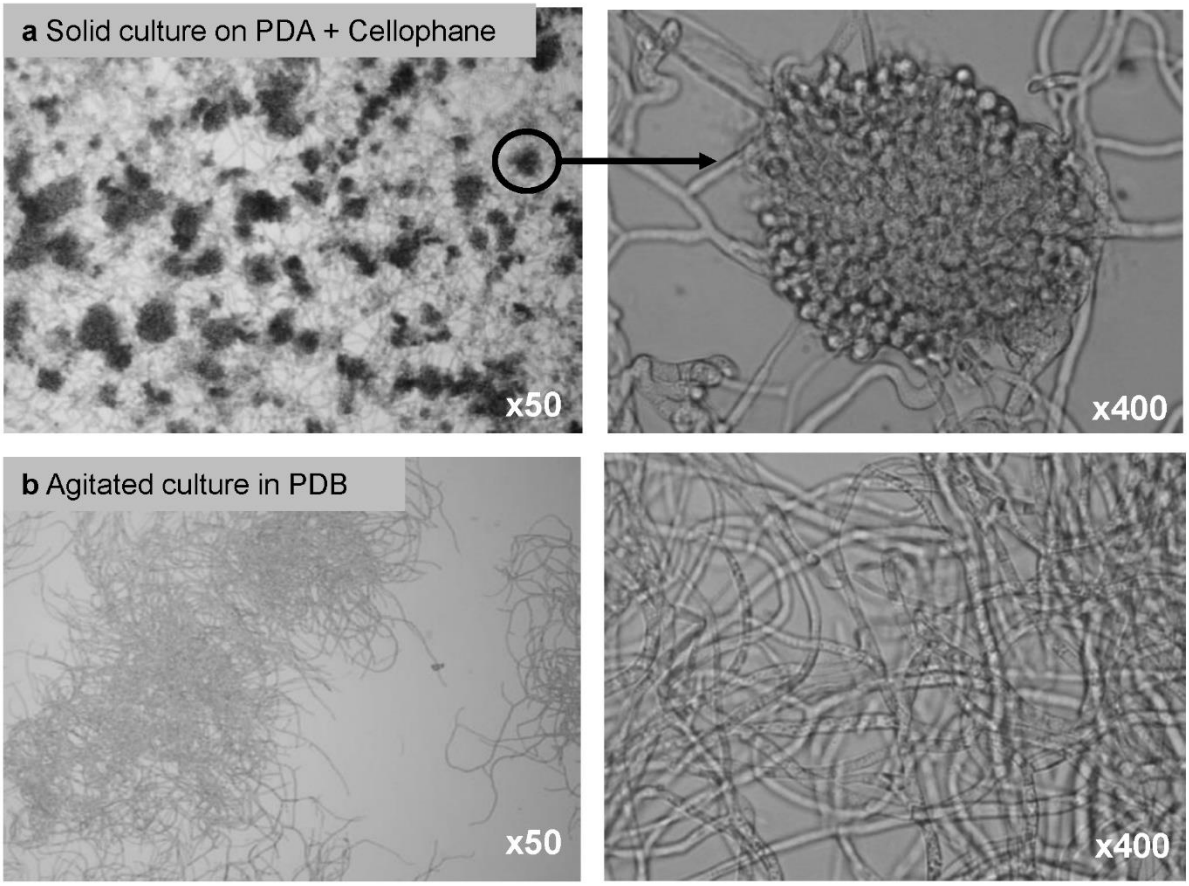

Fig. S2 Gene Ontology (GO) term enrichment analysis of genes differentially expressed in the infection cushion of *Botrytis cinerea*. Significantly (Fisher's exact test; p-values < 0.05) over-represented biological processes (BP) for the (a) 1,231 genes up-regulated in IC and (b) 1,422 genes down-regulated in IC. Enriched categories are classified according to p-values. Ratios inside the pie charts indicate the number of differentially expressed genes (underlined) relative to the total number of genes in each BP category (*italics*).

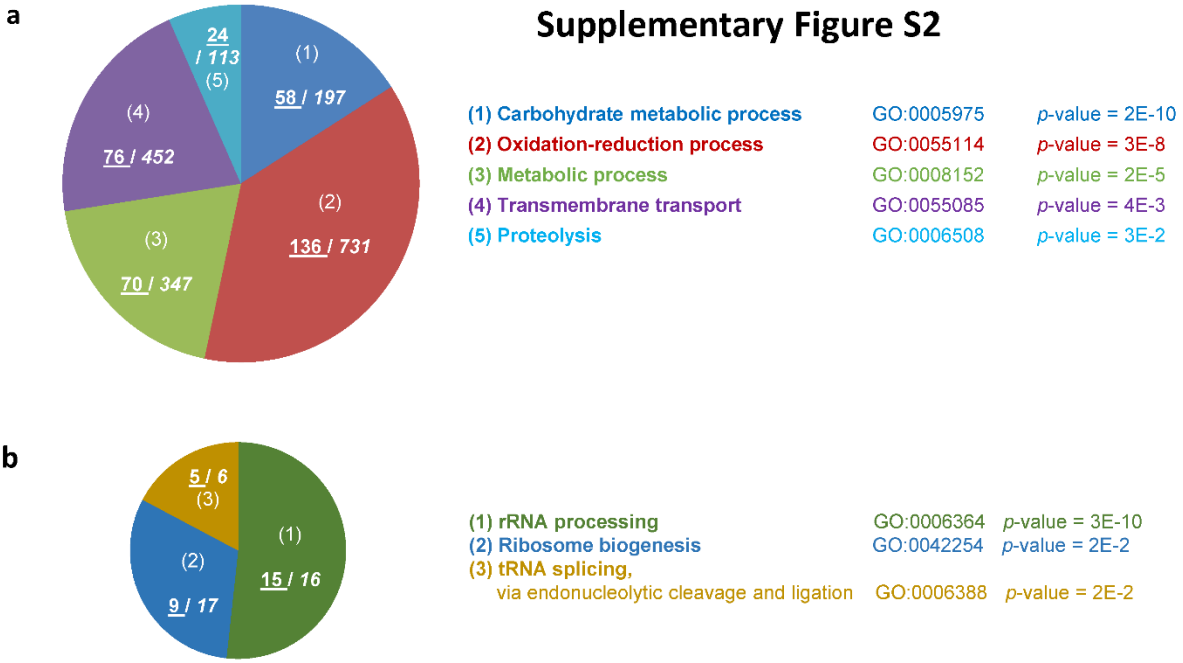

Fig. S3 Regulation of secondary metabolism biosynthesis key genes in the infection cushion of *Botrytis cinerea*. (a) Inventory of secondary metabolism (SM) biosynthesis key enzymes. The names, acronyms and number of genes coding for the SM key enzymes in *B. cinerea* are presented. (b) Hierarchical clustering of the expression of the 42 predicted SM key enzymes-encoding genes in IC (IC, 4 replicates) and control mycelium (Myc, 3 replicates). The normalized expression intensities are clustered and represented by color-coded squares; Shades of green and red depict down- and up-regulation in IC, respectively (Fold change $\leqslant$ -2 or $\geqslant$ 2 and FDR<0.05). Background corresponds to genes considered not expressed (with normalized intensities lower than the 99th percentile of random probes hybridization signals in all biological replicates).

Supplementary Figure S3

a

Key enzymes	Polyketide synthases	Non-ribosomal peptide synthetases	PKS-NRPS hybrids	Sesquiterpene cyclases	Diterpen cyclases	Dimethylallyl tryptophan synthases	Other
Acronym	PKS1, PKS2, PKS8 to PKS21	NRPS1 to NRPS9	PKS3 to PKS7	STC1 to STC5	DTC1 & DTC3	DMATS, DMATS2	CHS1, PAX1, PHS1
Number of genes	16	9	5	5	2	2	3

b

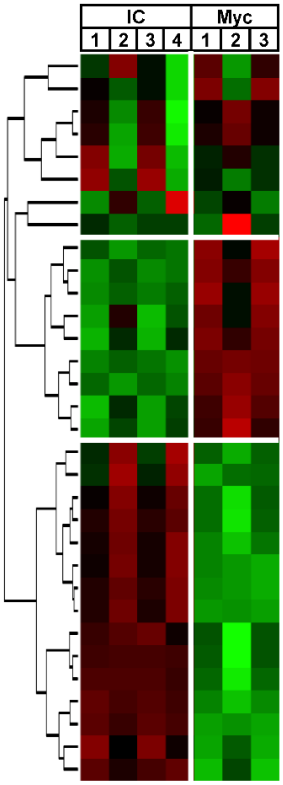

Gene ID	Chip reference	FC	FDR	Name	Description
Bcin05g06220	BofuT4_P135120	-1.0	8.2^{E-1}	*Bcpks15*	PKS
Bcin01g04920	BofuT4_P044420	-2.2	3.1^{E-1}	*Bcdtc1*	DTC
Bcin04g03550	BofuT4_P096230	-1.4	3.4^{E-1}	*Bcstc4*	STC
Bcin16g03570	BofuT4_P150070	-1.7	3.4^{E-1}	*Bcnrps3*	NRPS
Bcin16g01940	BofuT4_P033980	2.5	9.5^{E-1}	*Bcdmats1*	DMATS
Bcin01g11550	BofuT4_P085990	1.4	5.8^{E-1}	*Bcpks5*	PKS-NRPS
Bcin01g04560	BofuT4_P163490	1.2	6.4^{E-1}	*Bcphs1*	Phytoene synthase
Bcin02g02380	BofuT4_P109840	-1.3	4.7^{E-1}	*Bcnrps4*	NRPS
Bcin02g08830	BofuT4_P088290	-2.7	2.6^{E-2}	*Bcpks18*	PKS
Bcin14g01290	BofuT4_P059830	-10	4.1^{E-3}	*Bcpks11*	PKS
Bcin14g01300	BofuT4_P059820	-5.7	2.8^{E-2}	*Bcnrps9*	NRPS
Bcin12g00690	BofuT4_P120030	-1.6	1.2^{E-1}	*Bcnrps2*	NRPS
Bcin05g08400	BofuT4_P103050	-4.5	3.0^{E-2}	*Bcpks21*	PKS
Bcin01g11450	BC1G_15493	-24	7.0^{E-4}	*Bcnrps7*	NRPS
Bcin02g08770	BofuT4_P088370	-4.2	1.4^{E-3}	*Bcpks12*	PKS
Bcin08g02350	BofuT4_P130680	-2.5	2.3^{E-2}	*Bcstc2*	STC
Bcin03g04360	BofuT4_P020280	-3.4	2.9^{E-2}	*Bcpks3*	PKS-NRPS
Bcin04g00640	BofuT4_P085340	3.2	1.3^{E-1}	*Bcpks20*	PKS
Bcin01g03520	BofuT4_P162160	7.0	9.6^{E-2}	*Bcstc5*	STC
Bcin04g01390	BofuT4_P115630	2.8	3.3^{E-2}	*Bcnrps5*	NRPS
Bcin10g00040	BofuT4_P071110	8.5	1.7^{E-2}	*Bcpks7*	PKS-NRPS
Bcin08g00290	BofuT4_P119530	13	1.2^{E-2}	*Bcpks19*	PKS
Bcin11g02650	BofuT4_P037730	96	1.1^{E-2}	*Bcnrps8*	NRPS
Bcin08g03560	BofuT4_P132450	13	3.7^{E-3}	*Bcdtc3*	DTC
Bcin11g02700	BofuT4_P037790	50	5.2^{E-3}	*Bcpks4*	PKS-NRPS
Bcin13g02130	BofuT4_P125060	1.5	3.8^{E-2}	*Bcchs1*	Chalcone synthase
Bcin12g06390	BCexp3_CND15	4.2	2.7^{E-2}	*Bcbot2*	STC1
Bcin01g00090	BC1G_15837	6.6	1.1^{E-2}	*Bcboa9*	PKS9
Bcin01g00060	BC1G_16087	12	1.6^{E-3}	*Bcboa6*	PKS-NRPS(PKS6)
Bcin07g02920	BofuT4_P119030	10	5.9^{E-4}	*Bcpks8*	PKS
Bcin03g08050	BofuT4_P077210	5	2.4^{E-2}	*Bcpks13*	PKS
Bcin01g03730	BofuT4_P162470	1.9	1.3^{E-2}	*Bcnrps6*	NRPS
Bcin13g05830	BofuT4_P062370	Background		*Bcstc3*	STC
Bcin14g04900	BofuT4_P098370			*Bcdmats2*	DMATS
Bcin14g00600	BofuT4_P088990			*Bcpks1*	PKS
Bcin02g01680	BofuT4_P108860			*Bcpks2*	PKS
Bcin13g01510	BofuT4_P125860			*Bcpks10*	PKS
Bcin16g01830	BofuT4_P034180			*Bcpks14*	PKS
Bcin16g05040	BofuT4_P152140			*Bcpks16*	PKS
Bcin03g02010	BofuT4_P052990			*Bcpks17*	PKS
Bcin12g04980	BofuT4_P002220			*Bcnrps1*	NRPS
Bcin05g05670	BofuT4_P135790			*BcPax1*	PaxC-like terpen synthase

Fig. S4 Putative secondary metabolism gene clusters up-regulated in the infection cushion of *Botrytis cinerea*. (a) Hierarchical clustering of the expression of SM key enzymes-encoding genes and surrounding genes in IC (IC, 4 replicates) and control mycelium (Myc, 3 replicates). The normalized expression intensities are represented by color-coded squares; Shades of green and red depict down- and up-regulation in IC, respectively (Fold change $\leqslant$ -2 or $\geqslant$ 2 and FDR<0.05). (b) Genomic localization and representation of the 4 putative SM gene clusters DTC3, PKS7, PKS8 and PKS4-NRPS8. The genes up-regulated in IC are indicated in red and the supposed ends of each cluster are represented by the first neighboring genes non-regulated in IC (grey).

Supplementary Figure S4

a

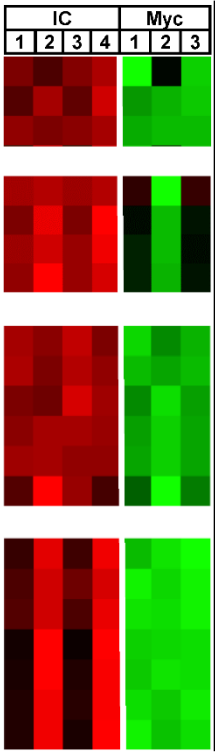

Gene ID	Chip reference	FC	FDR	Name	Description
Dtc3 cluster					
Bcin08g03550	BofuT4_P132440	3.4	2.9E-2	no	Hypothetical protein
Bcin08g03560	BofuT4_P132450	12	3.7E-3	***Bcdtc3***	**Diterpen cyclase**
Bcin08g03570	BofuT4_P132480	5.1	2.1E-4	no	**Cytochrome P450**
Pks7 cluster					
Bcin10g00030	BofuT4_P071050	2.9	1.1E-1	no	hypothetical protein
Bcin10g00010	BC1G_16236	16	3.1E-2	no	**hypothetical protein**
Bcin10g00020	BC1G_16237	19	1,6E-2	no	**MFS transporter**
Bcin10g00040	BofuT4_P071110	8.5	1.6E-2	***Bcpks7***	**PKS-NRPS hybrid**
Pks8 cluster					
Bcin07g02900	BofuT4_P118990	9.6	1.5E-3	no	**ABC transporter**
Bcin07g02920	BofuT4_P119030	10	5.9E-4	***Bcpks8***	**Polyketide synthase**
Bcin07g02930	BofuT4_P119040	2.9	2.9E-3	no	Hypothetical protein
Bcin07g02910	BofuT4_P119010	7.0	5.6E-4	no	EF-hand protein
Bcin07g02890	BofuT4_P118980	8.3	4.1E-4	no	Hypothetical protein
Bcin07g02940	BofuT4_P119050	2.0	2.4E-2	no	Kelch repeat-containing protein
Nrps8/Pks4 cluster					
Bcin11g02650	BofuT4_P037730	95	1.1E-2	***Bcnrps8***	**Non-ribosomal peptide synthetase**
Bcin11g02670	BofuT4_P037750	27	3.5E-3	no	**Dehydrogenase/reductase**
Bcin11g02700	BofuT4_P037790	50	5.2E-3	***Bcpks4***	**Polyketide synthase**
Bcin11g02690	BofuT4_P037770	51	2.7E-2	no	EF-hand protein
Bcin11g02640	BofuT4_P037720	56	2.0E-2	no	**Monooxygenase**
Bcin11g02680	BofuT4_P037760	131	1.6E-2	no	Acetyl-coA synthetase
Bcin11g02660	BofuT4_P037740	32	2.1E-2	no	**Methyl transferase**

b

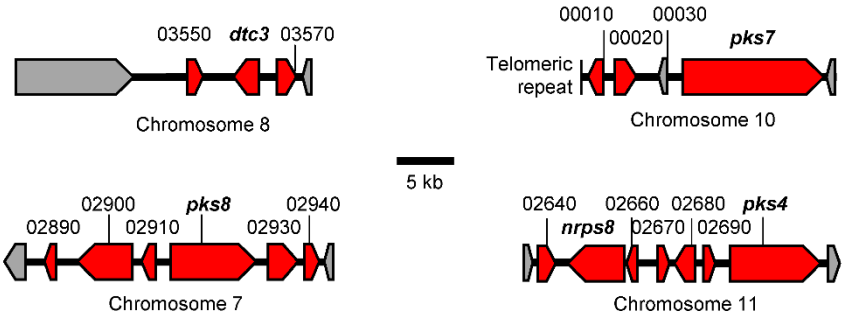

Fig. S5 Mutagenesis of genes encoding fasciclin-like proteins in *Botrytis cinerea*. (a) Creation of the *ΔBcflp1* deletion mutant (left) and Southern analysis (right). A split-marker strategy was used to replace the *Bcflp1* gene of the *B. cinerea* B05.10 strain by a hygromycin resistance gene (Hygro). The promoter and terminator DNA regions of *Bcflp1* (5'- and 3'-Flank) were inserted to the overlapping semi-replacement DNA cassettes in order to target them to the appropriate genomic locus. Homologous recombination (dashed lines) led to gene replacement. Genomic DNA of two hygromycin resistant clones (T2, T3) and the parental strain (WT) was digested by EcoRI (E) and subjected to Southern blot analysis using the 3'-flanking region as DNA probe (blue bar). (b) Creation of the *ΔBcflp2* deletion mutant (left) and Southern analysis (right). Following the same strategy described in (a), six transformants (T6-12) were analyzed by using the 5'-flanking region as DNA probe (green bar). (c) Creation of the *ΔBcflp1::ΔBcflp2* double deletion mutant (left) and Southern analysis (right). The same strategy described in (a) was used with the nourseothricin resistance gene (Nourseo) replacing the hygromycin resistance gene and the *ΔBcflp1* strain being the recipient strain for the transformation experiment. Three transformants (T) were analyzed by using the 3'-flanking region as DNA probe (blue bar). Gene replacements in the deletion strains were also verified by diagnostic PCR (data not shown).

Supplementary Figure S5

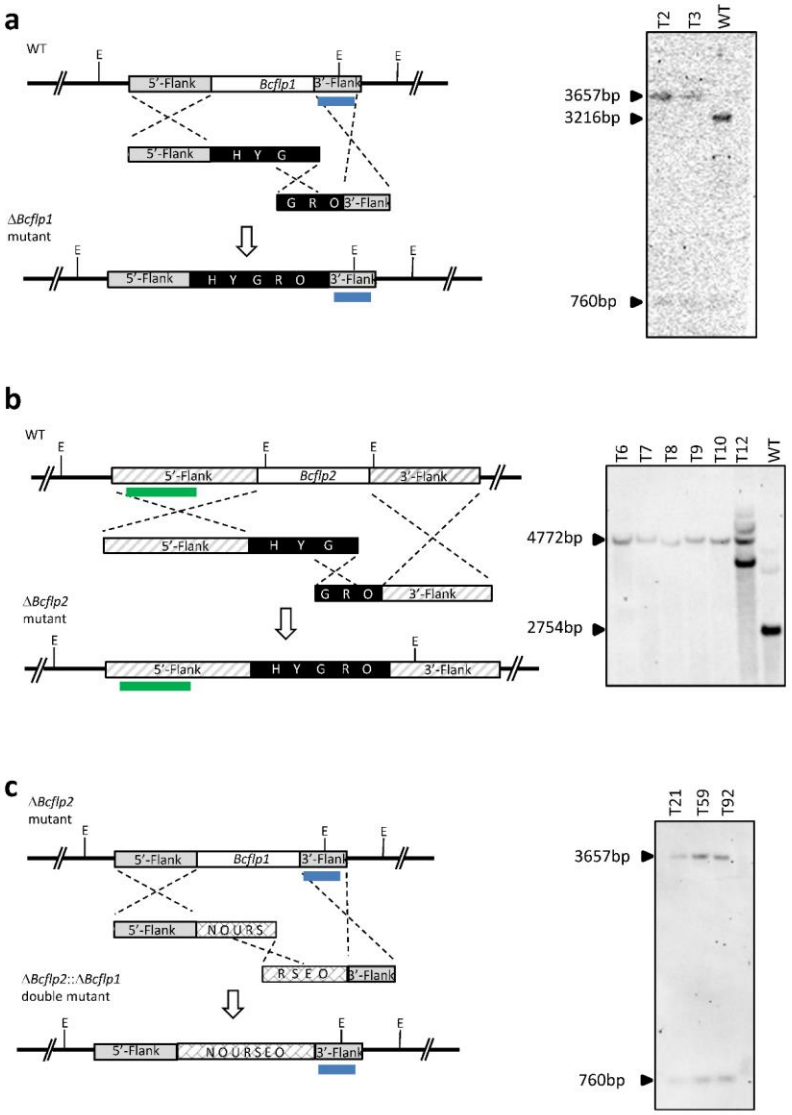

Fig. S6 Comparison of the *Botrytis cinerea* infection cushion (IC) transcriptome and the tran-scriptomes of four IC-deficient mutants. The transcriptomes (RNAseq) of four *B. cinerea* mutants impaired in the formation of IC were published (De Vallée *et al.*, 2019) and used for data comparison with the transcriptome of IC (this study). Genes repressed in these IC-deficient mutants were assumed to be induced in the infection cushion of the wild-type strain. This inverted correlation was confirmed for 40 genes among the top 100 upregulated genes in IC as they showed a common down-regulation in the four IC-deficient mutants.

De Vallée, A., Bally, P., Bruel, C., Chandat, L., Choquer, M., Dieryckx, C., *et al.* (2019) A Similar Secretome Disturbance as a Hallmark of Non-pathogenic Botrytis cinerea ATMT-Mutants? *Front Microbiol* **10**: 2829.

Supplementary Figure S6

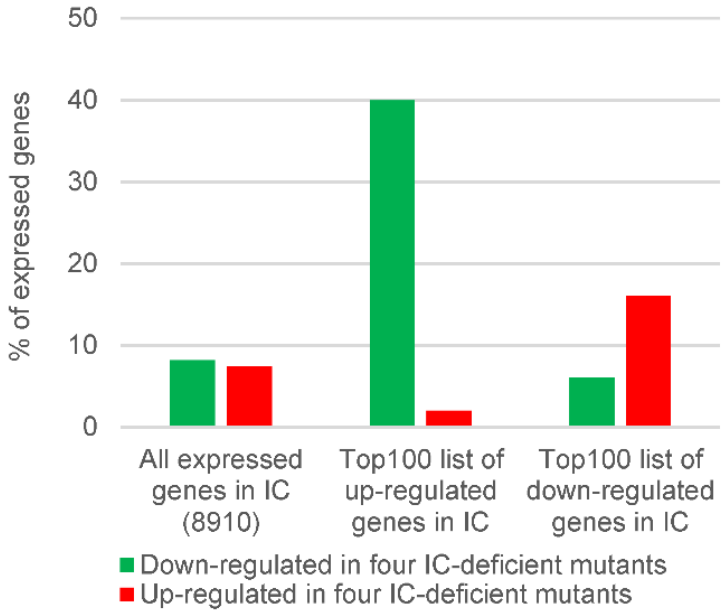

Legends of supplementary Tables

Table S1 Microarray analysis of the infection cushion of *Botrytis cinerea*. Table showing all Bcin genes (N=11,710) corresponding to the genome of B05.10 strain (ASM83294v1) structurally annotated by Van Kan *et al.* (2017) and available at http://fungi.ensembl.org/Botrytis_cinerea. N represents the total number of genes annotated on the genome and n represents the number of genes present on the chip. For each Bcin gene, the indicated Microarray chip reference is the corresponding gene from two previous genome annotations BofuT4 or BC1G (Amselem *et al*., 2011). Usual names were imported from the *Botrytis cinerea* Portal (http://botbioger.versailles.inra.fr/botportal/). 11,134 Bcin genes were analyzed by the Nimblegen Microarray chip which represent 95% of the published Bcin genes. They include Bcin genes up-regulated in IC (n=1,231), Bcin genes down-regulated in IC (n=1,422), Bcin genes expressed but not differentially regulated in IC (n=6,757), and Bcin genes not expressed in IC nor mycelium control (n=1,724). Fold change is the ratio between the mean of IC normalized intensities and the mean of mycelium control normalized intensities. ANOVA p-values were submitted to a False Discovery Rate correction (FDR). Transcripts with a corrected p-value < 0.05 and for which a fold change $\leqslant$ -2 or $\geqslant$ 2 was observed between the two conditions were considered to display significant differential expression. Normalized intensities are given for the infection cushion (4 biological replicates) and the mycelium control (3 biological replicates). Genes were considered not expressed when their normalized intensity was smaller than the 99th percentile of random probes hybridization signals in all biological replicates. For IC replicates 1 to 4, the 99th percentile of random probes hybridization signals was: 752, 572, 532 and 995, respectively. For mycelium replicates 1 to 3, the 99th percentile of random probes hybridization signals was: 752, 634 and 599, respectively (as determined by R software; R Core Team, 2019). Genes were manually sorted into 22 functional categories (see Table 1 for sources used for curation). Presence for a putative signal peptide was predicted using the SignalP 5.0 Server (Almagro Armenteros *et al*., 2019).

Almagro Armenteros, J.J., Tsirigos, K.D., Sønderby, C.K., Petersen, T.N., Winther, O., Brunak, S., *et al.* (2019) SignalP 5.0 improves signal peptide predictions using deep neural networks. *Nature Biotechnology* **37**: 420–423.

Amselem, J., Cuomo, C.A., van Kan, J.A.L., Viaud, M., Benito, E.P., Couloux, A., et al. (2011) Genomic Analysis of the Necrotrophic Fungal Pathogens *Sclerotinia sclerotiorum* and *Botrytis cinerea*. *PLoS Genetics* **7**: e1002230.

R Core Team (2019) R: A Language and Environment for Statistical Computing, Vienna, Austria: R Foundation for Statistical Computing.

Van Kan, J.A.L., Stassen, J.H.M., Mosbach, A., Van Der Lee, T.A.J., Faino, L., Farmer, A.D., et al. (2017) A gapless genome sequence of the fungus *Botrytis cinerea*: Gapless Genome Sequence of *B. cinerea*. *Molecular Plant Pathology* **18**: 75–89.

Table S2 *In vitro* RT-qPCR validation of microarray expression profiles from the infection cush-ion of *Botrytis cinerea*. Forty genes were chosen to test the differential expression recorded by the microarray analysis in the IC versus control mycelium. New biological replicates (n=3) were prepared and the expression of 24 up-regulated genes, 6 down-regulated genes and 10 non-regulated genes was measured by RT-qPCR. Gene expression levels were calculated following the $2^{-\Delta\Delta CT}$ method using constitutively expressed elongation factor *Bcef1α* as a reference (the use of the house-keeping actin (*BcactA*) and pyruvate dehydrogenase (*Bcpda1*) genes gave similar results; data not shown). Genes are ordered in the table according to their fold change in the microarray analysis and color codes corresponding to different fold change intensities are indicated. FC, fold change; FDR, false discovery rate; DE, differential expression.

Table S3 Up-accumulated proteins in the secretome of the infection cushion of *Botrytis cinerea*. (See legend of Table 2).

Table S3 corresponds to table 2 with additional information. SignalP and ApoplastP prediction softwares were respectively used to predict the presence of a signal peptide in these proteins sequence and the presence of these proteins in plant apoplast (http://apoplastp.csiro.au/; Sperschneider *et al.*, 2017). The microarray data (Chip reference, fold change and FDR) of these proteins-encoding genes are indicated. The behaviour of these proteins and corresponding genes in 4 IC-deficient mutants (De Vallée *et al*., 2019) are also indicated (with the fold change values (FC) and the associated p-values). up-regulated genes and up-accumulated proteins are colored in red. Down-regulated genes and down-accumulated proteins are colored in green.

De Vallée, A., Bally, P., Bruel, C., Chandat, L., Choquer, M., Dieryckx, C., *et al.* (2019) A Similar Secretome Disturbance as a Hallmark of Non-pathogenic Botrytis cinerea ATMT-Mutants? *Front Microbiol* **10**: 2829.

Sperschneider, J., Dodds, P.N., Singh, K.B., Taylor, J.M. (2018) APOPLASTP: prediction of effectors and plant proteins in the apoplast using machine learning. *New Phytologist*. **217**: 1764-1778.

Table S4 Primers used in this study for RT-qPCR analysis and constructs. For *Bcflp1* deletion construct, the 5'- and 3'- flanking regions of *Bcflp1* (1.115 kb and 0.624 kb) were amplified from *B. cinerea* genomic DNA using the primers pairs flp1-H1/flp1-H2 and flp1-H3/flp1-H4, respectively. flp1-H2 and flp1-H3 also contained sequences homologous to the hygromycin resistance cassette containing the hph gene under control of the oliC promoter. This cassette was generated using primers Hyg-H5 and Hyg-H6 and plasmid pFV8 as a template (Villalba *et al*., 2008). The purified amplicons were fused in a second round of PCR without any primer. Finally, a third step of PCR led to the amplification of two overlapping semi- replacement cassettes using nested primers flp1-H7/HYG-H7 and GRO-H8/flp1-H8 respectively. For *Bcflp2* deletion construct, the same strategy was applied using primers pairs flp2-H1/flp2-H2 for 5'- flanking region of Bcflp2 (1.962 kb) and flp2-H3/flp2-H4 for 3'- flanking region of Bcflp2 (1.468 kb) and resulted in two overlapping semi-replacement cassettes using nested primers flp2-H7/HYG-H7 and GRO-H8/flp2-H8 respectively. The development of double replacement mutants was achieved by transforming the previously generated *ΔBcflp2* mutant. Double deletion mutants *ΔBcflp2::ΔBcflp1* were constructed with the same strategy excepted that nourseothricin resistance was used instead of hygromycin. The 5'- and 3'- flanking regions of *Bcflp1* (1.095 kb and 0.56 kb) were amplified from *B. cinerea* genomic DNA using the primers pairs flp1-N1/flp1-N2 and flp1-N3/flp12-N4, respectively. The nourseothricin resistance cassette was amplified using flp1-N5 and flp1-N6 primers before fusion with the 5' and 3' flanking regions. Finally, two semi-cassettes were amplified using nested primers pairs flp1-N7/NOU-N7 and URS-N8/flp1-N8 respectively. *Bcflp1* replacement by the hygromycin cassette was verified using the primers pairs flp1-F5'/ hygro5' and hygro3'/flp1-F3' and the primers pairs flp1-N4/nour5' and nour3'/flp1-N1 for *Bcflp1* replacement by the nourseothricin cassette. *Bcflp2* replacement by the hygromycin cassette was verified using the primers pairs flp2-F5'/ hygro5' and hygro3'/flp2-F3'.

Villalba, F., Collemare, J., Landraud, P., Lambou, K., Brozek, V., Cirer, B., *et al.* (2008). Improved gene targeting in *Magnaporthe grisea* by inactivation of MgKU80 required for non-homologous end joining. *Fungal Genetics and Biology*. **45**: 68-75.